
Online Feature Updates Improve Online (Generalized) Label Shift Adaptation

Ruihan Wu^{*1} Siddhartha Datta^{*2} Yi Su³ Dheeraj Baby⁴ Yu-Xiang Wang⁴ Kilian Q. Weinberger⁵

Abstract

This paper addresses the prevalent issue of label shift in an online setting with missing labels, where data distributions change over time and obtaining timely labels is challenging. While existing methods primarily focus on adjusting or updating the final layer of a pre-trained classifier, we explore the untapped potential of enhancing feature representations using unlabeled data at test-time. Our novel method, Online Label Shift adaptation with Online Feature Updates (OLS-OFU), leverages self-supervised learning to refine the feature extraction process, thereby improving the prediction model. Theoretical analyses confirm that OLS-OFU reduces algorithmic regret by capitalizing on self-supervised learning for feature refinement. Empirical studies on various datasets, under both online label shift and generalized label shift conditions, underscore the effectiveness and robustness of OLS-OFU, especially in cases of domain shifts.

1. Introduction

The effectiveness of most supervised learning models relies on a key assumption that the training data and test data share the same distribution. However, this assumption rarely holds in real-world scenarios, leading to the phenomenon of *distribution shift* (Quiñonero-Candela et al., 2009; Amodei et al., 2016). Previous research has primarily focused on understanding distribution shifts in offline or batch settings, where a single shift occurs between the training and test distributions (Lin et al., 2002; Shimodaira, 2000; Zadrozny, 2004; Zhang et al., 2013; Lipton et al., 2018). In contrast, real-world applications often involve test data arriving in an *online* fashion, and the distribution shift can continuously evolve over time. Additionally, there is another challenging issue of *missing and delayed* feedback labels, stemming

from the online setup, where gathering labels for the streaming data in a timely manner becomes a challenging task.

To tackle the distribution shift problem, prior work often relies on additional assumptions regarding the nature of the shift, such as label shift or covariate shift (Schölkopf et al., 2012). In this paper, we focus on the common (*generalized*) label shift problem in an online setting with missing labels (Wu et al., 2021). Specifically, the learner is given a fixed set of labeled training data $D_0 \sim \mathcal{P}^{\text{train}}$ in advance and trains a model f_0 . During test-time, only a small batch of unlabelled test data $S_t \sim \mathcal{P}_t^{\text{test}}$ arrives in an online fashion ($t = 1, 2, \dots$). For the online label shift, we assume the label distribution $\mathcal{P}_t^{\text{test}}(y)$ may change over time t while the conditional distribution remains the same, i.e. $\mathcal{P}_t^{\text{test}}(x|y) = \mathcal{P}^{\text{train}}(x|y)$. For example, employing MRI image classifiers for concussion detection becomes challenging as label shifts emerge from seasonal variations in the image distribution. A classifier trained during skiing season may perform poorly when tested later, given the continuous change in image distribution between skiing and non-skiing seasons. In contrast to label shift, the *generalized* label shift relaxes the assumption of an unchanged conditional distribution on x given y . Instead, it assumes that there exists a transformation h of the covariate, such that the conditional distribution $\mathcal{P}_t^{\text{test}}(h(x)|y) = \mathcal{P}^{\text{train}}(h(x)|y)$ stays the same. Reiterating our example, consider an MRI image classifier that undergoes training and testing at different clinics, each equipped with MRI machines of varying hardware and software versions. As a result, the images may display disparities in brightness, resolution, and other characteristics. However, a feature extractor h exists, capable of mapping these variations to the same point in the transformed feature space, such that the conditional distribution $\mathcal{P}(h(x)|y)$ remains the same. In both settings, the goal of the learner is to adapt to the (generalized) label shift within the non-stationary environment, continually adjusting the model’s predictions in real-time.

Existing algorithms for online label shift adaptation (OLS) primarily adopt one of two approaches: either directly reweighting of the pretrained classifier f_0 , or re-training only the final linear layer of f_0 — while keeping the feature extractor frozen. Recent work (Sun et al., 2020; Wang et al., 2020; Liu et al., 2021; Niu et al., 2022) have demonstrated the potential for improving feature extractors, even during

^{*}Equal contribution ¹University of California, San Diego ²University of Oxford ³Google Deepmind ⁴University of California, Santa Barbara ⁵Cornell University. Correspondence to: Ruihan Wu <ruw076@ucsd.edu>.

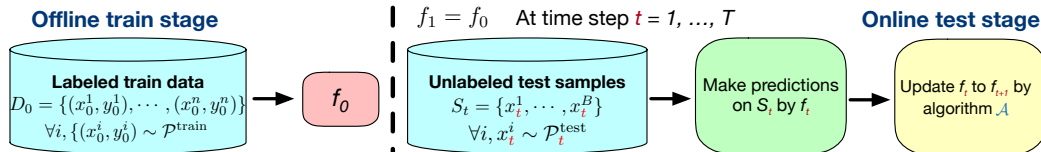


Figure 1. Overview of online distribution shift adaptation. We further assume $\mathcal{P}_t^{\text{test}}(x|y) = \mathcal{P}^{\text{train}}(x|y)$ for online label shift and assume the existence of an unknown feature mapping h such that $\mathcal{P}_t^{\text{test}}(h(x)|y) = \mathcal{P}^{\text{train}}(h(x)|y)$ for online generalized label shift.

test-time and in the absence of labeled data. We hypothesize that a similar effect can be harnessed in the context of (generalized) label shift, leading to the idea of *improving feature representation learning during testing*. In online label shift, updating the feature extractor offers two potential advantages. First, it utilizes the additional unlabeled samples, hence enhancing the sample efficiency of the feature extractor. Second, it enables the feature extractor to adapt to label shift, which is crucial to the learning process as the optimal feature extractor may depend on the underlying label distribution. Particularly in generalized label shift scenarios, where the feature transformation h is often unknown, the integration of extra unlabeled test samples facilitates the learning of h .

Building upon this insight, this paper introduces the *Online Label Shift adaptation with Online Feature Updates* (OLS-OFU) framework, aimed at enhancing feature representation learning in the context of online label shift adaptation. Specifically, each instantiation of OLS-OFU incorporates a self-supervised learning method associated with a loss function denoted as l_{ssl} for feature representation learning, and an online label shift adaptation (OLS) algorithm to effectively address distribution shift. However, it is worth pointing out that naively integrating feature extractor updates into traditional OLS algorithms will violate the underlying key assumptions of OLS algorithms (as we show in Section 3.1), hence compromising both performance and theoretical guarantees. To address this, our OLS-OFU is carefully designed to facilitate online feature updates within the OLS paradigm. At each time step, OLS-OFU executes a modified OLS algorithm, updates the feature extractor through self-supervised learning, and subsequently refines the final linear layer. This approach enables seamless online feature updates while preserving the theoretical guarantees inherent to the original OLS algorithms.

In addition to its ease of implementation and seamless integration with existing OLS algorithms, OLS-OFU also shows strong theoretical guarantee and empirical performance. Theoretically, we demonstrate that OLS-OFU effectively reduces the loss of the overall algorithm by leveraging self-supervised learning techniques to enhance the feature extractor, thereby improving predictions for test samples at each time step t . Empirical evaluations on both CIFAR-10 and CIFAR-10C datasets, considering both online label

shift and online generalized label shift scenarios, validate the effectiveness of OLS-OFU. It consistently outperforms its counterpart OLS methods across various datasets and distribution shift settings, underscoring its robustness across different scenarios.

2. Problem Setting & Related Work

We start with some basic notations. Let Δ^{K-1} be the probability simplex. Let $f : \mathcal{X} \rightarrow \Delta^{K-1}$ denote a classifier. Given an input x from domain \mathcal{X} , $f(x)$ outputs a probabilistic prediction over K classes. For example, f can be the output from the softmax operation after any neural network. If we reweight a model f by a vector $p \in \mathbb{R}^K$, we refer to this model as $g(\cdot; f, p)$ with g denotes the method of reweighting. For any two vectors p and q , p/q denotes the element-wise division.

Online distribution shift adaptation. The effectiveness of any machine learning model f relies on a common assumption that the train data D_0 and test data D_{test} are sampled from the same distribution, i.e., $\mathcal{P}^{\text{train}} = \mathcal{P}^{\text{test}}$. However, this assumption is often violated in practice, which leads to *distribution shift*. This can be caused by various factors, such as data collection bias and changes in the data generation process. Moreover, once a well-trained model f_0 is deployed in the real world, it moves into the testing phase, which is composed of a sequence of time periods or time steps. The test distribution at time step t , $\mathcal{P}_t^{\text{test}}$, from which test data x_t is sampled, may vary over time. One example is that an MRI image classifier might be trained on MRI images collected during skiing season (which may have a high frequency of head concussions) but tested afterward (when the frequency of concussion is lower). The test stage can last several months until the next classifier is trained. During this test period, the distribution of MRI images may undergo continuous changes, transitioning between non-skiing and skiing seasons.

As the test-time distribution changes over time, the challenge lies in how to adjust the model continuously from f_{t-1} to f_t in an online fashion to adapt to the current distribution $\mathcal{P}_t^{\text{test}}$. We call this problem *online distribution shift adaptation* and illustrate it in Figure 1. Given a total of T steps in the online test stage, we define the average loss for any online algorithm \mathcal{A} through the loss of the sequence of

models $f_t, t \in [T]$ that are produced from \mathcal{A} , i.e.,

$$L(\mathcal{A}; \mathcal{P}_1^{\text{test}}, \dots, \mathcal{P}_T^{\text{test}}) = \frac{1}{T} \sum_{t=1}^T \ell(f_t; \mathcal{P}_t^{\text{test}}), \quad (1)$$

where $\ell(f; \mathcal{P}) = \mathbb{E}_{(x,y) \sim \mathcal{P}} \ell_{\text{sup}}(f(x), y)$ and ℓ_{sup} is the loss function, for example, 0-1 loss or cross-entropy loss for classification tasks.

If we have knowledge of $\mathcal{P}_t^{\text{test}}$ or have enough samples from $\mathcal{P}_t^{\text{test}}$, then the problem reduces to offline distribution shift for each single time step t . Alternatively, if we have a few labeled samples, the problem can be treated as classical online learning, and we can run stochastic gradient descent at the end of every time step t to meet certain theoretical guarantees. However, dealing with very few unlabeled samples or even a single sample x_t is more realistic yet technically highly non-trivial. An effective algorithm under this scenario has to utilize information from all historical data (train data D_0 , validation data D'_0 and test data up to time t), as well as previously deployed models $f_{0,1,\dots,t-1}$. In this paper, we consider the challenging scenario where at each time step t , only a *small batch of unlabeled samples* $S_t = \{x_t^1, \dots, x_t^B\}$ is received. We formalize the algorithm \mathcal{A} as: $\forall t \in [T]$,

$$f_t := \mathcal{A}(\{S_1, \dots, S_{t-1}\}, \{f_1, \dots, f_{t-1}\}, D_0, D'_0). \quad (2)$$

In contrast to the classical online learning setup, this scenario presents a significant challenge as classical online learning literature usually relies on having access to either full or partial knowledge of the loss at each time step, i.e., $\ell_{\text{sup}}(f(x_t), y_t)$. In this setting, however, only a batch of unlabeled samples is provided at each time step. This lack of access to label information and loss values presents a significant challenge in accurately estimating the true loss defined in Equation 1.

Related work have studied the online distribution shift adaptation under various distribution shift assumptions, such as label shift (Wu et al., 2021; Bai et al., 2022; Baby et al., 2023) and covariate shift (Zhang et al., 2023). In this paper, we focus on online (generalized) label shift adaptation.

Online label shift adaptation. Online label shift assumes

$$\forall t \in [T], \mathcal{P}_t^{\text{test}}(x|y) = \mathcal{P}^{\text{train}}(x|y),$$

while the marginal distribution of the label $\mathcal{P}_t^{\text{test}}(y)$ changes over time. This assumption is most typical when the label y is the causal variable and the feature x is the observation (Schölkopf et al., 2012). The aforementioned example of concussion detection from MRI images fits this scenario, where the presence or absence of a concussion (label) causes the observed MRI image features. Most previous methods tackle this problem through a non-trivial reduction to the classical online learning problem. Consequently, most of

the online label shift algorithms (Wu et al., 2021; Bai et al., 2022; Baby et al., 2023) study the theoretical guarantee of the algorithm via the convergence of the regret function, which could be either static regret or dynamic regret. In previous studies, the hypothesis class \mathcal{F} of the prediction function f is typically chosen in one of two ways. The first approach involves defining \mathcal{F} as a family of post-hoc reweightings of f_0 , with the parameter space comprising potential reweight vectors. Examples within this category include ROGD (Wu et al., 2021), FTH (Wu et al., 2021), and FLHFTL (Baby et al., 2023). The second approach defines \mathcal{F} as a family of functions that share the same parameters in f_0 except the last linear layer, such as UOGD (Bai et al., 2022) and ATLAS (Bai et al., 2022).

Online generalized label shift adaptation. In the context of MRI image classification, where head MRI images serve as the feature x , variations in software or hardware across different clinics' MRI machines can introduce discrepancies in image characteristics like brightness, contrast, and resolution. In such scenarios, the conditional probability distribution $\mathcal{P}(x|y)$ is no longer invariant. However, when a feature extractor h is robust enough, it can map images into a feature space where the images from different machines have the same distributions $\mathcal{P}(h(x)|y)$ in the transformed feature space. The concept of generalized label shift, as introduced in Tachet des Combes et al. (2020), formalizes this by postulating the existence of an unknown function h , such that $\mathcal{P}(h(x)|y)$ remains invariant. The primary challenge in this context is to find the underlying transformation h . Building upon this, online generalized label shift assumes that, there exists an unknown function h such that

$$\forall t \in [T], \mathcal{P}_t^{\text{test}}(h(x)|y) = \mathcal{P}^{\text{train}}(h(x)|y).$$

Self-supervised learning. Inspired by the extensive body of work in semi-supervised learning (Grandvalet & Bengio, 2004b; Lee et al., 2013; Laine & Aila, 2016; Gidaris et al., 2018; Miyato et al., 2018) and unsupervised representation learning (Chen et al., 2020a; He et al., 2020; Grill et al., 2020; He et al., 2022), self-supervised learning (SSL) techniques have emerged as promising tools for improving feature extraction from unlabeled data, such as applications in image classification. Likewise, when dealing with online label shift adaptation, it is crucial to leverage the unlabeled test samples $S_1 \cup \dots \cup S_{t-1}$ obtained from previous time steps. Ideally, these unlabeled samples could improve the feature representation learning and ultimately lead to better prediction for the test samples S_t at time step t .

In this paper, we narrow our focus on three particular SSL techniques in the evaluation for classification tasks: rotation degree prediction (Gidaris et al., 2018; Sun et al., 2020), entropy minimization (Grandvalet & Bengio, 2004b; Wang et al., 2020) and MoCo (He et al., 2020; Chen et al., 2020b;

2021). It is important to note that this concept extends beyond these three SSL techniques, and the incorporation of more advanced SSL techniques has the potential to further elevate the performance. Specifically, rotation degree prediction involves initially rotating a given image by a specific degree from the set $\{0, 90, 180, 270\}$ and the classifier is required to determine the degree by which the image has been rotated. Entropy minimization utilizes a minimum entropy regularizer, with the motivation that unlabeled examples are mostly beneficial when classes have a small overlap. MoCo is a more advanced representation learning technique, using a query and momentum encoder to learn representations from unlabeled data by maximizing the similarity of positive pairs and minimizing the similarity of negative pairs. More details of these SSL techniques are given in Appendix E.8.

3. Method

We introduce a novel online label shift adaptation algorithm OLS-OFU, that leverages self-supervised learning (SSL) to improve representation learning, while maintaining theoretical guarantees. This approach is general and can be seamlessly integrated with any existing online label shift (OLS) method. We show both theoretical and empirical improvement of OLS-OFU. Moreover, we demonstrate their effectiveness in addressing the more challenging problem of online generalized label shift adaptation.

3.1. Online Label Shift Adaptation with Online Feature Updates

Main ideas. Before formally introducing the algorithm, we would like to discuss two crucial design principles about where to place the update feature extractor through SSL, inspired by the analysis of OLS methods in the literature. These principles are essential for maintaining both the theoretical guarantees and potential empirical performance.

Principle 1: at time step t , the feature extractor update using samples S_t should occur after the OLS updates.

The main idea of ROGD, UOGD, and ATLAS is to construct an unbiased estimator for the gradient $\nabla_f \ell(f_t; \mathcal{P})$ using a batch of samples $S_t \sim \mathcal{P}_t^{\text{test}}$. The estimator has the form of

$$\sum_{y \in \mathcal{Y}} s_t[y] \cdot \nabla_f \mathbb{E}_{x \sim \mathcal{P}^{\text{train}}(\cdot|y)} \ell_{\text{sup}}(f_t(x), y), \quad (3)$$

where the randomness of s_t depends on samples S_t as constructed and is an unbiased estimator for the label marginal distribution q_t . The following proposition introduces a necessary condition of f_t to ensure the unbiased property of the above estimator and the proof is given at Appendix B.

Proposition 1. *If f_t is not independent of the samples S_t , the gradient estimator in Equation 3 is not guaranteed to be an unbiased estimator of the gradient $\nabla_f \ell(f_t; \mathcal{P})$.*

From the proposition, it is necessary to ensure f_t is independent of S_t . Thus, the update of the feature extractor in f_t (using SSL) using samples S_t should occur after the online label shift (OLS) method is updated with S_t .

Principle 2: the last linear layer should be re-trained using the train set D_0 after the feature extractor update.

The key observation here is that a label-shifted distribution $\mathcal{P}_t^{\text{test}}(y|x)$ is an exact post-hoc reweight of $\mathcal{P}^{\text{train}}(y|x)$:

$$\begin{aligned} \mathcal{P}_t^{\text{test}}(y|x) &= \frac{\mathcal{P}_t^{\text{test}}(y)}{\mathcal{P}_t^{\text{test}}(x)} \mathcal{P}_t^{\text{test}}(x|y) = \frac{\mathcal{P}_t^{\text{test}}(y)}{\mathcal{P}_t^{\text{test}}(x)} \mathcal{P}^{\text{train}}(x|y) \\ &= \frac{\mathcal{P}_t^{\text{test}}(y)}{\mathcal{P}_t^{\text{test}}(x)} \frac{\mathcal{P}^{\text{train}}(x)}{\mathcal{P}^{\text{train}}(y)} \mathcal{P}^{\text{train}}(y|x) \propto \frac{\mathcal{P}_t^{\text{test}}(y)}{\mathcal{P}^{\text{train}}(y)} \mathcal{P}^{\text{train}}(y|x). \end{aligned}$$

Another observation is that f_0 trained from D_0 could be a good approximation of $\mathcal{P}^{\text{train}}(y|x)$. These two observations motivate approaches like ROGD, FTH, and FLHFTL to opt for the hypothesis f to be a post-hoc reweight of the pre-trained model f_0 . In the context of our framework, these methods need to be adapted slightly. Instead of reweighting the original model f_0 directly, they should reweight a model within the updated feature extractor. This reweighted model should still approximate the original train data distribution $\mathcal{P}^{\text{train}}(y|x)$, which can be achieved by re-training the last linear layer using the initial train data D_0 .

Algorithm details. The two principles together motivate our final algorithm: *Online Label Shift adaptation with Online Feature Updates* (OLS-OFU; Algorithm 1), which requires a self-supervised learning loss ℓ_{ssl} and an online label shift adaptation algorithm (OLS) that either reweights the offline pre-trained model f_0 or updates the last linear layer¹. In the training stage, we train f_0 by minimizing the supervised and self-supervised loss together defined on train data. In the test stage, OLS-OFU comprises three steps at each time step t : (1) running the refined version of OLS, which we refer to as OLS-R, (2) updating the feature extractor, and (3) re-training the last linear layer. The details of these three steps are elaborated below.

(1) Running the Revised OLS. At the beginning of the time t , we use f_t'' to denote the model within the latest feature extractor and the re-trained linear model (using data $\{S_0, \dots, S_{t-1}\}$). The high level idea of our framework centers on substituting the pre-trained model f_0 used in existing OLS methods with our updated model f_t'' , which we call *Revised OLS*. To provide an overview, we examine common OLS methods (FLHFTL, FTH, ROGD, UOGD, and ATLAS) and identify two primary usecases of f_0 . Firstly, all OLS methods rely on an unbiased estimator s_t of the

¹As pointed out in Section 2, this is relatively general as most previous online label shift algorithms belong to these two categories.

Algorithm 1 Online label shift adaptation with online feature updates (OLS-OFU).

Require: An online label shift adaptation algorithm OLS, a self-supervised learning loss ℓ_{ssl} . A pre-trained model f_0 and initialize $f_1 = f'_1 := f_0$.

for $t = 1, \dots, T$ **do**

Input at time t : Samples $S_1 \cup \dots \cup S_t$, models $\{f_1, \dots, f_t\}$, train set D_0 and validation set D'_0 .

1. Run the revised version of OLS, that is, OLS-R, and get f'_{t+1} . (Algorithm 2 is the revised FLHFTL.)

2. Update the feature extractor θ^{feat} in f'_{t+1} by Equation 4. Replace θ^{feat} in f'_{t+1} by θ^{feat} .

3. Re-train the last linear layer by Equation 5. Calibrate the model $f(\cdot | \theta^{\text{feat}}, \theta^{\text{linear}})$ by temperature calibration on D'_0 and get the calibrated model f''_{t+1} .

Output at time t : For the reweighting OLS methods, denote the latest reweighting vector from Step 1 is p_{t+1} and we define $f_{t+1} := g(\cdot; f'_{t+1}, p_{t+1})$; else, we define $f_{t+1} := f'_{t+1}$.

end for

Algorithm 2 Revised FLHFTL for online feature updates (FLHFTL-R); See the original version in (Baby et al., 2023).

Require: Online regression oracle ALG.

for $t = 1, \dots, T$ **do**

Input at time t : Samples $S_1 \cup \dots \cup S_t$, models $\{f_1, \dots, f_t\}$, intermediate models $\{f'_1, \dots, f'_t\}$, the validation set D'_0 , the train label marginal $q_0 := \mathcal{P}^{\text{train}}(y)$.

1. Compute the unbiased estimator for label marginal distribution: $s_t = \frac{1}{|S_t|} \sum_{x_t \in S_t} C_{f'_t, D'_0}^{-1} f''_t(x_t)$ ▷ In the original FLHFTL, it is f_0 rather than f'_t .

2. Compute $\tilde{q}_{t+1} := \text{ALG}(s_1, \dots, s_t)$

3. Let f'_{t+1} be a reweighting version of f''_t by the weight $\left(\frac{\tilde{q}_{t+1}[k]}{q_0[k]} : k = 1, \dots, K\right)$ ▷ In the original FLHFTL, it is f_0 rather than f'_t .

Output at time t : f'_{t+1} .

end for

label distribution q_t and f_0 is a part of the estimator. Secondly, the hypothesis f is either reweighted based on f_0 or only the last linear layer in f_0 is updated. To illustrate the revised OLS formally, Algorithm 2 showcases the specific modifications applied to FLHFTL as an example. Further details regarding the revisions for ROGD, FTH, UOGD, and ATLAS can be found in Appendix C. We use f'_{t+1} to denote the model after running the revised OLS.

(2) Updating the Feature Extractor. We now introduce how to utilize the SSL loss ℓ_{ssl} to update the feature extractor based on any incoming batch of unlabeled test data S_t at timestep t . Specifically, let θ^{feat} denote the parameters of

the feature extractor in f'_{t+1} . The update of θ^{feat} at time t is given by:

$$\theta^{\text{feat}}_{t+1} := \theta^{\text{feat}}_t - \eta \cdot \nabla_{\theta^{\text{feat}}} \ell_{\text{ssl}}(S_t; f'_{t+1}). \quad (4)$$

Then we update the feature extractor in f'_{t+1} with θ^{feat} .

(3) Re-training Last Linear Layer. With the updated feature extractor θ^{feat} , it is important to re-train the last linear layer θ^{linear} to align with the new feature extractor. The re-training starts from random initialization, while the feature extractor remains frozen. The training objective of θ^{linear} is to minimize the average cross-entropy loss over train data D_0 . We denote the model with the frozen feature extractor θ^{feat} as $f(\cdot | \theta^{\text{feat}}, \theta^{\text{linear}})$. The objective for re-training last linear layer can be written as follows:

$$\theta^{\text{linear}}_{t+1} := \arg \min_{\theta^{\text{linear}}} \sum_{(x,y) \in D_0} \ell_{\text{ce}} \left(f(x | \theta^{\text{feat}}, \theta^{\text{linear}}), y \right). \quad (5)$$

We calibrate the model $f(\cdot | \theta^{\text{feat}}, \theta^{\text{linear}})$ by temperature calibration (Guo et al., 2017) using the validation set D'_0 and denote the model after calibration as f''_{t+1} . This re-training step is essential to ensure the model is a calibrated model of estimating $\mathcal{P}^{\text{train}}(y|x)$ rather than other distributions.

Output at time t . Finally, we define f_{t+1} for the next time step prediction. For the reweighting OLS methods (ROGD, FTH, FLHFTL), denote the latest reweighting vector from Step 1 is p_{t+1} and define $f_{t+1} := g(\cdot; f'_{t+1}, p_{t+1})$. For those which optimize the last linear layer (UOGD, ATLAS), we define $f_{t+1} := f'_{t+1}$ – as stated in Principle 2 in Section 3.1, the f'_t including retrained last linear layer serves specially for the reweighting OLS method.

Batch accumulation for SSL that needs large batches.

The loss of SSL such as contrastive learning (Chen et al., 2020a; He et al., 2020) is defined from a batch of data and the effective batch is necessary to be large. We introduce a simple variant of Algorithm 1: we process Step 2-3 every BA time steps by the samples collected in the period.

3.2. Performance Guarantee

The original OLS methods exhibit theoretical guarantees in terms of regret convergence for online label shift setting, where $\mathcal{P}_t^{\text{test}}(x|y) = \mathcal{P}^{\text{train}}(x|y)$ is invariant. With the incorporation of the additional online feature update step, OLS-OFU demonstrates analogous theoretical results. By comparing the theoretical results between OLS and OLS-OFU, we can gain insights into potential enhancements from OLS to OLS-OFU. Due to limited space, we provide the theoretical results pertaining to FLHFTL-OFU here, and present the theoretical results for ROGD-OFU, FTH-OFU, UOGD-OFU, and ATLAS-OFU in Appendix D.

Theorem 2. [Regret convergence for FLHFTL-OFU]

Suppose we choose the OLS subroutine in Algorithm 2

to be FLHFTL from [Baby et al. \(2023\)](#). Let $f_t^{\text{flhftl-ofu}}$ be the output at time step $t - 1$ from Algorithm 1, that is $g(\cdot; f_t'', \frac{q_t}{q_0})$. Let σ be the smallest among the minimum singular values of invertible confusion matrices $\{C_{f_1'', D'_0}, \dots, C_{f_T'', D'_0}\}$. Then under Assumptions 1 and 2 in [Baby et al. \(2023\)](#), FLHFTL-OFU has the guarantee below:

$$\begin{aligned} & \mathbb{E} \left[\frac{1}{T} \sum_{t=1}^T \ell(f_t^{\text{flhftl-ofu}}; \mathcal{P}_t^{\text{test}}) - \frac{1}{T} \sum_{t=1}^T \ell(g(\cdot; f_t'', \frac{q_t}{q_0}); \mathcal{P}_t^{\text{test}}) \right] \\ & \leq O \left(\frac{K^{1/6} V_T^{1/3}}{\sigma^{2/3} T^{1/3}} + \frac{K}{\sigma \sqrt{T}} \right), \end{aligned} \quad (6)$$

where $V_T := \sum_{t=1}^T \|q_t - q_{t-1}\|_1$, K is the number of classes, and the expectation is taken w.r.t. randomness in the revealed co-variables. This result is attained without prior knowledge of V_T .

To ease comparison, we state the guarantee for the original OLS method FLHFTL ([Baby et al., 2023](#)):

$$\begin{aligned} & \mathbb{E} \left[\frac{1}{T} \sum_{t=1}^T \ell(f_t^{\text{flhftl}}; \mathcal{P}_t^{\text{test}}) \right] - \frac{1}{T} \sum_{t=1}^T \ell(g(\cdot; f_0, \frac{q_t}{q_0}); \mathcal{P}_t^{\text{test}}) \\ & \leq O \left(\frac{K^{1/6} V_T^{1/3}}{\sigma^{2/3} T^{1/3}} + \frac{K}{\sigma \sqrt{T}} \right), \end{aligned} \quad (7)$$

Recall that the objective function for the online label shift problem is defined as the average loss in Equation 1. Both theorems establish the convergence in terms of this average loss. In the event that f_t'' ($t \in [T]$) from the online feature updates yield improvements:

$$\mathbb{E} \left[\frac{1}{T} \sum_{t=1}^T \ell(g(\cdot; f_t'', \frac{q_t}{q_0}); \mathcal{P}_t^{\text{test}}) \right] < \frac{1}{T} \sum_{t=1}^T \ell(g(\cdot; f_0, \frac{q_t}{q_0}); \mathcal{P}_t^{\text{test}}), \quad (8)$$

then it guarantees that the loss of FLHFTL-OFU will converge to a smaller value, resulting in enhanced performance compared to FLHFTL. We substantiate this improvement through empirical evaluation in Section 4. For other OLS methods such as ROGD-OFU, FTH-OFU, UOGD-OFU, and ATLAS-OFU, a similar analysis can be derived and we present them in Appendix D.

3.3. Online Feature Updates Improve Online Generalized Label Shift Adaptation

When we have knowledge of the feature map h under generalized label shift, the problem simplifies to the classical online label shift scenario. However, the more challenging situation arises when h remains unknown. Due to the violation of the label shift assumption, standard OLS methods can perform arbitrarily bad. Fortunately, existing research in test-time training (TTT) ([Sun et al., 2020](#); [Wang et al., 2020](#);

[Liu et al., 2021](#); [Niu et al., 2022](#)) demonstrates that feature updates driven by SSL align the source and target domains in feature space. When the source and target domains achieve perfect alignment, such feature extractor effectively serves as the feature map h as assumed in generalized label shift. Therefore, the sequence of feature extractors in f_1, \dots, f_T generated by Algorithm 1 progressively approximates the underlying h . This suggests that, compared to the original OLS, OLS with online feature updates (Algorithm 1) experiences a milder violation of the label shift assumption within the feature space and is actually expected to have better performance in the setting of online generalized label shift. Indeed, as demonstrated in Section 4, we can observe significant improvements in OLS-OFU compared to standard OLS for online generalized label shift.

4. Experiment

In this section, we empirically evaluate how OLS-OFU improves the original OLS methods on both online label shift and online generalized label shift². The experiment is performed on CIFAR-10 ([Krizhevsky et al., 2009](#)), STL10 ([Coates et al., 2011](#)), CINIC ([Darlow et al., 2018](#)), EuroSAT ([Helber et al., 2019](#)), and CIFAR-10C ([Hendrycks & Dietterich, 2019](#)). We systematically vary the distribution shift processes and self-supervised learning (SSL) techniques to assess the effectiveness of the proposed method.

4.1. Experiment Set-up

Dataset and Label Shift Settings. For online label shift, we evaluate the efficacy of our algorithm on CIFAR-10 ([Krizhevsky et al., 2009](#)), STL10 ([Coates et al., 2011](#)), CINIC ([Darlow et al., 2018](#)), and EuroSAT ([Helber et al., 2019](#)), which have 10 categories of images. For each dataset, we split the original train set into the offline train (i.e., D_0) and validation sets (i.e., D'_0) following a ratio of 4 : 1. At the online test unlabeled batches are sampled from the test set. For online generalized label shift, the offline train and validation sets are the same CIFAR-10 images. The test unlabeled batches are drawn from CIFAR-10C, a benchmark with the same objects as CIFAR-10 but with various types of corruption. We experiment with three types of corruptions with CIFAR-10C: Gaussian noise, Fog and Pixelate.

We follow [Bai et al. \(2022\)](#) and [Baby et al. \(2023\)](#) to simulate the online label distribution shift with two shift patterns: Sinusoidal shift and Bernoulli shift. Specifically, given two label distribution vectors q and q' , we simulate the label marginal distributions at time t as a weighted combination of them: $q_t := \alpha_t q + (1 - \alpha_t) q'$. In Sinusoidal shift, $\alpha_t = \sin \frac{i\pi}{L}$ (periodic length $L = \sqrt{T}$, $i = t \bmod L$) while

²Code released at https://anonymous.4open.science/r/online_label_shift_with_online_feature_updates-3A1F/.

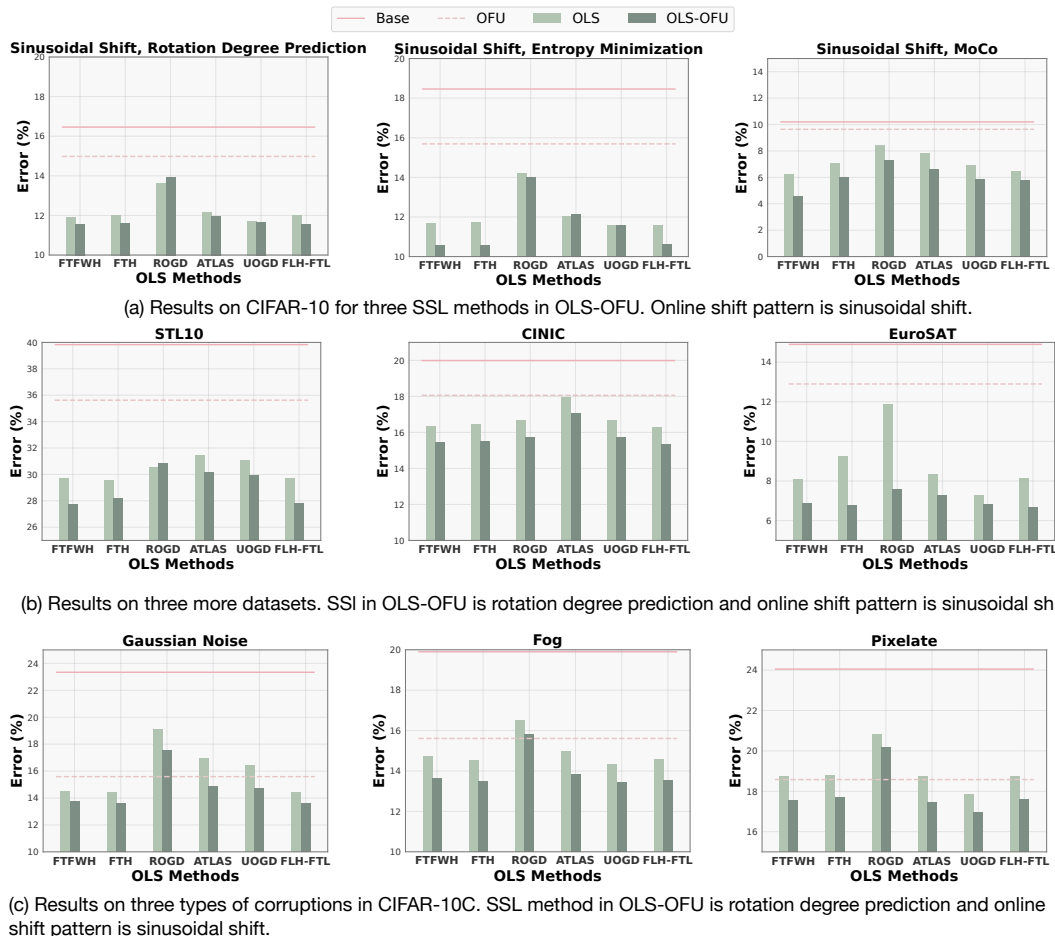


Figure 2. Evaluation of OLS and OLS-OFU.

in Bernoulli shift, α_t is a random bit (either 0 or 1), where the bit switches $\alpha_t = 1 - \alpha_{t-1}$ with probability $p = 1 - \frac{1}{\sqrt{T}}$. In our experiments, we set the initial distribution vector q and q' with $\frac{1}{K}(1, \dots, 1)$ and $(1, 0, \dots, 0)$. To sample the batch test data at time t , we first sample a batch of labels (not revealed to the learner) according to q_t . Then given each label we can sample an image from the test set, and collect this batch of images without labels as S_t . We experiment with $T = 1000$ and batch size $B = 10$ at each time step, following Baby et al. (2023).

Evaluation Metric. We report the average error during test, i.e., $\frac{1}{TB} \sum_{t=1}^T \sum_{x_t \in S_t} \mathbb{1}(f_t(x_t) \neq y_t)$, where $(x_t, y_t) \sim \mathcal{P}_t^{\text{test}}$, to approximate $\frac{1}{T} \sum_{t=1}^T \ell(f_t; \mathcal{P}_t^{\text{test}})$ for the evaluation efficiency. This is valid for large T due to its exponential concentration rate by the Azuma–Hoeffding inequality.

Baselines and OLS Methods. We perform an extensive evaluation of 6 OLS methods in the literature: FTFWH, FTH, ROGD, UOGD, ATLAS, and FLHFTL. We further report the performance of our method OLS-OFU (Algorithm 1) applied on top of each OLS. OLS-OFU is instantiated with 3 common SSL methods introduced in Section 2: rotation degree prediction, entropy minimization, and MoCo.

We run the batch accumulation variant of Algorithm 1 for MoCo and set BA=50; please see the ablation for the selection of BA in Appendix E.8.1. Additionally, we report two baseline scores, Base and OFU. The Base uses the fixed pre-trained model f_0 to predict the labels at all time steps. The second is online feature updates (OFU) only, where at time step t we only update the features (Step 2 in Algorithm 1) without utilizing OLS algorithms.

4.2. Results

Main Results: comparison between OLS-OFU and baselines under online (generalized) label shift. Figure 2(a) shows the performance comparison between OLS-OFU, implemented with *three* SSL methods, and their corresponding OLS counterparts on CIFAR-10 under the scenario of *classical online label shift*. Figure 2(b) shows the results on *three more datasets* with SSL technique in OLS-OFU being rotation degree prediction. The online shift pattern in the setting of Figure 2(a-b) is sinusoidal shift. From Figure 2(a-b), we can observe that OLS-OFU outperforms all other baselines. Notably, OLS-OFU, when integrated with three SSL methods, consistently outperforms their counterpart

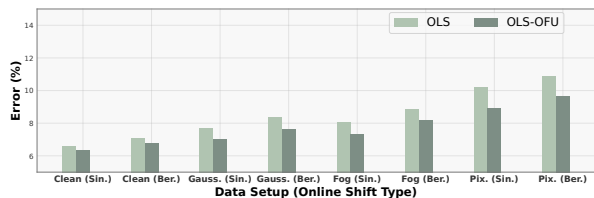


Figure 3. Empirical examination for the holdness of Equation 8. Clean denotes the experiment on CIFAR-10 and others denotes the corruption type. They are paired with two online shift patterns: Sinusoidal and Bernoulli.

OLS method across all of the OLS methods. This emphasizes the importance of improving representation learning within label shift adaptation and underscores the robustness of our framework OLS-OFU. Results for Bernoulli shift in Appendix E.3 show similar conclusion.

Furthermore, we report the performance of OLS-OFU in the context of *online generalized label shift*. In this scenario, the test images exhibit three types of domain shifts in CIFAR-10C — Gaussian noise, Fog, and Pixelation—with mild severity. We present the result under Sinusoidal shift with the SSL method used in OLS-OFU as rotation degree prediction. Similar to the scenario of online label shift, the superior performance of OLS-OFU compared with Base, OFU, and OLS demonstrates its superiority (Figure 2(c)). Particularly, OLS-OFU consistently outperforms the original OLS methods by an even larger gap than the one occurring at the classic label shift setting. We hypothesize that the inclusion of SSL methods within OLS-OFU aids the learning of the unknown mapping h inherent in the generalized label shift assumption. As evaluated in Sun et al. (2020), the label shift assumption in the feature space of θ_t^{feat} is violated milder than the one of θ_0^{feat} — the more severe violation of θ_0^{feat} explains why some OLS methods perform even worse than OFU. Results for other SSL methods and online shift patterns show a similar pattern in Appendix E.4.

Moreover, as an *ablation study* of OLS-OFU, the comparison between OLS-OFU and either OLS or OFU individually underscores the specific benefits of both the OFU and OLS modules in addressing the challenges posed by the online (generalized) label shift problem.

Empirical validation of Equation 8. In Section 3.2, we argued that when the inequality in Equation 8 holds, the loss of FLHFTL-OFU exhibits a tighter upper bound compared to FLHFTL. Figure 3 presents the RHS (corresponds to OLS) and LHS (corresponds to OLS-OFU with SSL loss as rotation degree prediction) of Equation 8. We perform the study over eight different settings and varies the domain shift and online shift patterns. It is evident that OLS-OFU yields improvements on the *baseline* of the regret as shown in Equation 8. Appendix E.6 validates this inequality for other SSL techniques. We further examine how the improvement

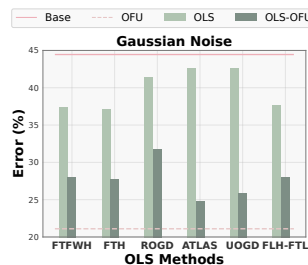


Figure 4. Results on CIFAR-10C for a high level of severity.

from Equation 8 (RHS - LHS) is correlated the improvement from OLS to OLS-OFU. For each OLS method, we compute the Pearson coefficient (within the range of $[-1, 1]$) between these two terms across all experimental setups (varying dataset, online shift pattern, and SSL methods). The calculated coefficients are 0.70, 0.76, 0.54, 0.63, 0.58, and 0.75 when OLS is FTFWH, FTH, ROGD, ATLAS, UOGD, or FLHFTL, respectively. These values indicate strong positive correlations, underscoring how improvements in regret align with empirical performance improvements.

Results on CIFAR-10C with higher severity. We evaluate all methods on CIFAR-10C with higher severity of domain shifts. Figure 4 shows the results when the test images are corrupted by Gaussian noise³. Comparing with Figure 2(c), it is clear that as the severity increases, OLS-OFU enlarges the performance gap compared to OLS. However, it might be worth pointing out that neither OLS nor OLS-OFU are better than OFU. This is because the severe violation of the label shift assumption — noted that even OFU cannot reduce the violation under an acceptable level (still get 20% error rate), which gives inferior performance of OLS-OFU compared to OFU, as the adaptation to distribution shift deviates significantly.

5. Conclusion

We focus on online (generalized) label shift adaptation and present a novel framework *Online Label Shift adaptation with Online Feature Updates* (OLS-OFU), which harnesses the power of self-supervised learning to enhance feature representations dynamically during testing, leading to improved predictive models and better test time performance.

Discussion and future work. One promising direction is to extend the idea of this paper to online covariate shift, for example, the algorithm in Zhang et al. (2023) freezes the feature extractor and only updates the linear layer. Another possible direction is to consider a more realistic domain shift scenario within the generalized label shift setting — domain shift types may vary over time or be even more challenging, such as shifting from cartoon images to realistic images.

³Please refer to Appendix E.5 for results involving higher levels of severity, other corruption types, and SSL techniques.

Acknowledgements

RW and KQW are supported by grants from LinkedIn, DARPA Geometries of Learning, and the National Science Foundation NSF (1934714). RW is also supported by grants from the National Science Foundation NSF (2241100), Army Research Office ARO MURI (W911NF2110317), and Office of Naval Research ONR (N00014-20-1-2334).

References

- Alexandari, A., Kundaje, A., and Shrikumar, A. Maximum likelihood with bias-corrected calibration is hard-to-beat at label shift adaptation. In *International Conference on Machine Learning*, pp. 222–232. PMLR, 2020.
- Amodei, D., Olah, C., Steinhardt, J., Christiano, P., Schulman, J., and Mané, D. Concrete problems in ai safety. *arXiv preprint arXiv:1606.06565*, 2016.
- Arazo, E., Ortego, D., Albert, P., O’Connor, N. E., and McGuinness, K. Pseudo-labeling and confirmation bias in deep semi-supervised learning. In *2020 International Joint Conference on Neural Networks (IJCNN)*. IEEE, 2020.
- Azizzadenesheli, K., Liu, A., Yang, F., and Anandkumar, A. Regularized learning for domain adaptation under label shifts. In *International Conference on Learning Representations*, 2019.
- Baby, D. and Wang, Y.-X. Optimal dynamic regret in proper online learning with strongly convex losses and beyond. In *International Conference on Artificial Intelligence and Statistics*, pp. 1805–1845. PMLR, 2022.
- Baby, D., Garg, S., Yen, T.-C., Balakrishnan, S., Lipton, Z. C., and Wang, Y.-X. Online label shift: Optimal dynamic regret meets practical algorithms. *To appear at Advances in Neural Information Processing Systems*, 2023.
- Bai, Y., Zhang, Y.-J., Zhao, P., Sugiyama, M., and Zhou, Z.-H. Adapting to online label shift with provable guarantees. *Advances in Neural Information Processing Systems*, 35: 29960–29974, 2022.
- Besbes, O., Gur, Y., and Zeevi, A. Non-stationary stochastic optimization. *Operations research*, 63(5):1227–1244, 2015.
- Chen, T., Kornblith, S., Norouzi, M., and Hinton, G. A simple framework for contrastive learning of visual representations. In *International conference on machine learning*, pp. 1597–1607. PMLR, 2020a.
- Chen, X., Fan, H., Girshick, R., and He, K. Improved baselines with momentum contrastive learning. *arXiv preprint arXiv:2003.04297*, 2020b.
- Chen, X., Xie, S., and He, K. An empirical study of training self-supervised vision transformers. In *2021 IEEE/CVF International Conference on Computer Vision (ICCV)*, pp. 9620–9629, Los Alamitos, CA, USA, oct 2021. IEEE Computer Society. doi: 10.1109/ICCV48922.2021.00950. URL <https://doi.ieeecomputersociety.org/10.1109/ICCV48922.2021.00950>.
- Coates, A., Ng, A., and Lee, H. An Analysis of Single Layer Networks in Unsupervised Feature Learning. In *AISTATS*, 2011. https://cs.stanford.edu/~acoates/papers/coatesleeng_aistats_2011.pdf.
- Darlow, L. N., Crowley, E. J., Antoniou, A., and Storkey, A. J. Cinic-10 is not imagenet or cifar-10, 2018.
- Garg, S., Wu, Y., Balakrishnan, S., and Lipton, Z. C. A unified view of label shift estimation. *arXiv preprint arXiv:2003.07554*, 2020.
- Garg, S., Erickson, N., Sharpnack, J., Smola, A., Balakrishnan, S., and Lipton, Z. Rlsbench: Domain adaptation under relaxed label shift. In *International Conference on Machine Learning (ICML)*, 2023.
- Gidaris, S., Singh, P., and Komodakis, N. Unsupervised representation learning by predicting image rotations. In *International Conference on Learning Representations*, 2018. URL <https://openreview.net/forum?id=S1v4N210->.
- Grandvalet, Y. and Bengio, Y. Semi-supervised learning by entropy minimization. In Saul, L., Weiss, Y., and Bottou, L. (eds.), *Advances in Neural Information Processing Systems*, volume 17. MIT Press, 2004a. URL https://proceedings.neurips.cc/paper_files/paper/2004/file/96f2b50b5d3613adf9c27049b2a888c7-Paper.pdf.
- Grandvalet, Y. and Bengio, Y. Semi-supervised learning by entropy minimization. *Advances in neural information processing systems*, 17, 2004b.
- Gretton, A., Smola, A., Huang, J., Schmittfull, M., Borgwardt, K., and Schölkopf, B. Covariate shift by kernel mean matching. *Dataset shift in machine learning*, 3(4): 5, 2009.
- Grill, J.-B., Strub, F., Altché, F., Tallec, C., Richemond, P., Buchatskaya, E., Doersch, C., Avila Pires, B., Guo, Z., Gheshlaghi Azar, M., et al. Bootstrap your own latent—a new approach to self-supervised learning. *Advances in neural information processing systems*, 33:21271–21284, 2020.

- Guo, C., Pleiss, G., Sun, Y., and Weinberger, K. Q. On calibration of modern neural networks. In *International conference on machine learning*, pp. 1321–1330. PMLR, 2017.
- He, K., Fan, H., Wu, Y., Xie, S., and Girshick, R. Momentum contrast for unsupervised visual representation learning. In *Proceedings of the IEEE/CVF conference on computer vision and pattern recognition*, pp. 9729–9738, 2020.
- He, K., Chen, X., Xie, S., Li, Y., Dollár, P., and Girshick, R. Masked autoencoders are scalable vision learners. In *Proceedings of the IEEE/CVF conference on computer vision and pattern recognition*, pp. 16000–16009, 2022.
- Helber, P., Bischke, B., Dengel, A., and Borth, D. Eurosat: A novel dataset and deep learning benchmark for land use and land cover classification. *IEEE Journal of Selected Topics in Applied Earth Observations and Remote Sensing*, 12(7):2217–2226, 2019. doi:10.1109/JSTARS.2019.2918242.
- Hendrycks, D. and Dietterich, T. Benchmarking neural network robustness to common corruptions and perturbations. *arXiv preprint arXiv:1903.12261*, 2019.
- Hoffman, J., Darrell, T., and Saenko, K. Continuous manifold based adaptation for evolving visual domains. In *Proceedings of the IEEE Conference on Computer Vision and Pattern Recognition*, pp. 867–874, 2014.
- Huang, J., Gretton, A., Borgwardt, K., Schölkopf, B., and Smola, A. Correcting sample selection bias by unlabeled data. In *Advances in neural information processing systems*, volume 19, pp. 601–608. Citeseer, 2006.
- Krizhevsky, A., Hinton, G., et al. Learning multiple layers of features from tiny images. 2009.
- Laine, S. and Aila, T. Temporal ensembling for semi-supervised learning. *arXiv preprint arXiv:1610.02242*, 2016.
- Lee, D.-H. Pseudo-label: The simple and efficient semi-supervised learning method for deep neural networks. *ICML 2013 Workshop: Challenges in Representation Learning*, 2013.
- Lee, D.-H. et al. Pseudo-label: The simple and efficient semi-supervised learning method for deep neural networks. In *Workshop on challenges in representation learning, ICML*, volume 3, pp. 896. Atlanta, 2013.
- Lin, Y., Lee, Y., and Wahba, G. Support vector machines for classification in nonstandard situations. *Machine learning*, 46(1):191–202, 2002.
- Lipton, Z., Wang, Y.-X., and Smola, A. Detecting and correcting for label shift with black box predictors. In *International conference on machine learning*, pp. 3122–3130. PMLR, 2018.
- Liu, Y., Kothari, P., Van Delft, B., Bellot-Gurlet, B., Mordan, T., and Alahi, A. Ttt++: When does self-supervised test-time training fail or thrive? *Advances in Neural Information Processing Systems*, 34:21808–21820, 2021.
- Miyato, T., Maeda, S.-i., Koyama, M., and Ishii, S. Virtual adversarial training: a regularization method for supervised and semi-supervised learning. *IEEE transactions on pattern analysis and machine intelligence*, 41(8):1979–1993, 2018.
- Mullapudi, R. T., Chen, S., Zhang, K., Ramanan, D., and Fatahalian, K. Online model distillation for efficient video inference. In *Proceedings of the IEEE/CVF International Conference on Computer Vision*, pp. 3573–3582, 2019.
- Niu, S., Wu, J., Zhang, Y., Chen, Y., Zheng, S., Zhao, P., and Tan, M. Efficient test-time model adaptation without forgetting. In *International conference on machine learning*, pp. 16888–16905. PMLR, 2022.
- Quiñonero-Candela, J., Sugiyama, M., Lawrence, N. D., and Schwaighofer, A. *Dataset shift in machine learning*. Mit Press, 2009.
- Saerens, M., Latinne, P., and Decaestecker, C. Adjusting the outputs of a classifier to new a priori probabilities: a simple procedure. *Neural Computation*, 14(1):21–41, 2002.
- Schölkopf, B., Janzing, D., Peters, J., Sgouritsa, E., Zhang, K., and Mooij, J. On causal and anticausal learning. *arXiv preprint arXiv:1206.6471*, 2012.
- Shalev-Shwartz, S. 2012.
- Shimodaira, H. Improving predictive inference under covariate shift by weighting the log-likelihood function. *Journal of statistical planning and inference*, 90(2):227–244, 2000.
- Sun, Y., Wang, X., Liu, Z., Miller, J., Efros, A., and Hardt, M. Test-time training with self-supervision for generalization under distribution shifts. In *International conference on machine learning*, pp. 9229–9248. PMLR, 2020.
- Tachet des Combes, R., Zhao, H., Wang, Y.-X., and Gordon, G. J. Domain adaptation with conditional distribution matching and generalized label shift. *Advances in Neural Information Processing Systems*, 33:19276–19289, 2020.
- Wang, D., Shelhamer, E., Liu, S., Olshausen, B., and Darrell, T. Tent: Fully test-time adaptation by entropy minimization. *arXiv preprint arXiv:2006.10726*, 2020.

- Wu, R., Guo, C., Su, Y., and Weinberger, K. Q. Online adaptation to label distribution shift. *Advances in Neural Information Processing Systems*, 34:11340–11351, 2021.
- Xie, Q., Luong, M.-T., Hovy, E., and Le, Q. V. Self-training with noisy student improves imagenet classification. In *2020 IEEE/CVF Conference on Computer Vision and Pattern Recognition (CVPR)*, pp. 10684–10695, 2020. doi: 10.1109/CVPR42600.2020.01070.
- Zadrozny, B. Learning and evaluating classifiers under sample selection bias. In *Proceedings of the Twenty-First International Conference on Machine Learning*, pp. 114, 2004.
- Zhang, K., Schölkopf, B., Muandet, K., and Wang, Z. Domain adaptation under target and conditional shift. In *International Conference on Machine Learning*, pp. 819–827. PMLR, 2013.
- Zhang, Y.-J., Zhang, Z.-Y., Zhao, P., and Sugiyama, M. Adapting to continuous covariate shift via online density ratio estimation. *arXiv preprint arXiv:2302.02552*, 2023.

A. Further Related Work

Offline distribution shift and domain shift. Offline label shift and covariate shift have been studied for many years. Some early work (Saerens et al., 2002; Lin et al., 2002) assumes the knowledge of how the distribution is shifted. Later work (Shimodaira, 2000; Zadrozny, 2004; Huang et al., 2006; Gretton et al., 2009; Lipton et al., 2018; Alexandari et al., 2020; Azizzadenesheli et al., 2019; Garg et al., 2020) relaxes this assumption and estimates this knowledge from unlabeled test data. A recent work by (Garg et al., 2023) considers a relaxed version of offline label shift problem where the class-conditionals can change between train and test domains in a restrictive way. Extending their results to the case of relaxed online version of generalized label shift is an interesting future direction.

Online distribution shift with provable guarantees. There has been several work modeling online distribution shift as the classic online learning problem (Wu et al., 2021; Bai et al., 2022; Baby et al., 2023; Zhang et al., 2023), which leverage the classical online learning algorithms (Shalev-Shwartz, 2012; Besbes et al., 2015; Baby & Wang, 2022) to bound the static or dynamic regret. However, none of them updates the feature extractor in a deep learning model but only the last linear layer or the post-hoc linear reweighting vectors. Our proposed method OLS-OFU utilizes the deep learning SSL to improve the feature extractor, which brings better performance.

Domain shift adaptation within online streaming data. When we consider the most authentic online learning setup where the learner only receives the unlabeled samples, the most representative idea is test-time training (Sun et al., 2020; Wang et al., 2020; Liu et al., 2021; Niu et al., 2022), which utilizes a (deep learning) self-supervised loss to online update the model. However, it focuses on how to adapt to a *fixed* domain shifted distribution from online streaming data and is not designed for how to adapt to continuous distribution changes during the test stage, while our algorithm concentrates the later problem. Besides test-time training, Hoffman et al. (2014) and (Mullapudi et al., 2019) study the online domain shift for specific visual applications.

Algorithm 3 Revised ROGD for online feature updates ROGD-R. See the original version in Equation 7 and Equation 8 in (Wu et al., 2021).

Require: Learning rate η .

for $t = 1, \dots, T$ **do**

Input at time t : Samples $S_1 \cup \dots \cup S_t$, models $\{f_1, \dots, f_t\}$, and intermediate model $\{f''_1, \dots, f''_t\}$ from step 3 in Algorithm 1, the validation set D'_0 , the training label marginal $q_0 := \mathcal{P}^{\text{train}}(y)$.

1. Compute the unbiased estimator for label marginal distribution:

$$s_t = \frac{1}{|S_t|} \sum_{x_t \in S_t} C_{f''_t, D'_0}^{-1} f''_t(x_t). \quad \triangleright \text{In the original ROGD, it is } f_0 \text{ rather than } f''_t.$$

2. Grab the weight p_t from f_t .

3. Update $p_{t+1} := \text{Proj}_{\Delta^{K-1}} [p_t - \eta \cdot J_p(p_t)^\top s_t]$,

where $J_p, f''_t(p_t) = \frac{\partial}{\partial p} (1 - \text{diag}(C_{f''_t, D_0, p}))|_{p=p_t}$, and let f_{t+1} be a reweighting version of f''_t by the weight

$$\left(\frac{p_{t+1}[k]}{q_0[k]} : k = 1, \dots, K \right) \quad \triangleright \text{In the original ROGD, it is } f_0 \text{ rather than } f''_t.$$

Output at time t : f'_{t+1} .

end for

Algorithm 4 Revised FTH for online feature updates (FTH-R). See the original version in Equation 9 in (Wu et al., 2021).

for $t = 1, \dots, T$ **do**

Input at time t : Samples $S_1 \cup \dots \cup S_t$, models $\{f_1, \dots, f_t\}$, and intermediate model $\{f''_1, \dots, f''_t\}$ from step 3 in Algorithm 1, the validation set D'_0 , the train label marginal $q_0 := \mathcal{P}^{\text{train}}(y)$.

1. Compute the unbiased estimator for label marginal distribution:

$$s_t = \frac{1}{|S_t|} \sum_{x_t \in S_t} C_{f_t, D'_0}^{-1} f''_t(x_t). \quad \triangleright \text{In the original FTL, it is } f_0 \text{ rather than } f''_t.$$

2. Compute $p_{t+1} = \frac{1}{t} \sum_{\tau=1}^t s_\tau$

3. Let f_{t+1} be a reweighting version of f''_t by

$$\text{the weight } \left(\frac{p_{t+1}[k]}{q_0[k]} : k = 1, \dots, K \right) \quad \triangleright \text{In the original FTL, it is } f_0 \text{ rather than } f''_t.$$

Output at time t : f'_{t+1} .

end for

Algorithm 5 Revised UOGD for online feature updates (UOGD-R). See the original version in Equation 9 in (Bai et al., 2022).

Require: The learning rate η .

for $t = 1, \dots, T$ **do**

Input at time t : Samples $S_1 \cup \dots \cup S_t$, models $\{f_1, \dots, f_t\}$, and intermediate model $\{f_1'', \dots, f_t''\}$ from step 3 in Algorithm 1, the validation set D'_0 , the train label marginal $q_0 := \mathcal{P}^{\text{train}}(y)$.

1. Compute the unbiased estimator for label marginal distribution:

$$s_t = \frac{1}{|S_t|} \sum_{x_t \in S_t} C_{f_t'', D'_0}^{-1} f_t''(x_t). \quad \triangleright \text{In the original UOGD, it is } f_0 \text{ rather than } f_t''.$$

2. Grab the weight w_t from the last linear layer of f_t .

3. Update $w_{t+1} := w_t - \eta \cdot \frac{\partial}{\partial w} J_w(w_t)^\top s_t$, where $J_w(w_t) = \frac{\partial}{\partial w} (\hat{R}_t^1(w), \dots, \hat{R}_t^K(w))|_{w=w_t}$,

$$\hat{R}_t^k(w) = \frac{1}{|D_0^k|} \sum_{(x,y) \in D_0^k} \ell_{\text{ce}}(f(x|\theta_t^{\text{feat}}, \theta^{\text{linear}} = w), y), D_0^k \text{ denotes the set of data with label } k \text{ in } D_0. \quad \triangleright \text{In the original UOGD, it is } \theta_0^{\text{feat}} \text{ rather than } \theta_t^{\text{feat}}.$$

4. Let f_{t+1} be $f(\cdot|\theta_t^{\text{feat}}, w_{t+1})$.

Output at time t : f'_{t+1} .

end for

Algorithm 6 Revised ATLAS for online feature updates (ATLAS-R). See the original version in Equation 9 in (Bai et al., 2022).

Require: The learning rate pool \mathcal{H} with size N ; Meta learning rate ε ; $\forall i \in [N], p_{1,i} = 1/N$ and $w_{1,i} = \theta_{f_0}^{\text{linear}}$.

for $t = 1, \dots, T$ **do**

Input at time t : Samples $S_1 \cup \dots \cup S_t$, models $\{f_1, \dots, f_t\}$, and intermediate model $\{f_1'', \dots, f_t''\}$ from step 3 in Algorithm 1, the validation set D'_0 , the train label marginal $q_0 := \mathcal{P}^{\text{train}}(y)$.

1. Compute the unbiased estimator for label marginal distribution:

$$s_t = \frac{1}{|S_t|} \sum_{x_t \in S_t} C_{f_t, D'_0}^{-1} f_t''(x_t). \quad \triangleright \text{In the original ATLAS, it is } f_0 \text{ rather than } f_t''.$$

for $i \in [N]$ **do**

2. Update $w_{t+1,i} := w_{t,i} - \eta_i \cdot \frac{\partial}{\partial w} J_w(w_{t,i})^\top s_t$, where

$$J_w(w_{t,i}) = \frac{\partial}{\partial w} (\hat{R}_t^1(w), \dots, \hat{R}_t^K(w))|_{w=w_{t,i}},$$

$$\hat{R}_t^k(w) = \frac{1}{|D_0^k|} \sum_{(x,y) \in D_0^k} \ell_{\text{ce}}(f(x|\theta_t^{\text{feat}}, w), y), D_0^k \text{ denotes the set of data$$

with label k in D_0 .

\triangleright In the original ATLAS, it is θ_0^{feat} rather than θ_t^{feat} .

end for

3. Update weight p_{t+1} according to $p_{p_{t,i}} \propto \exp(-\varepsilon \sum_{\tau=1}^{t-1} \hat{R}_\tau(\mathbf{w}_{\tau,i}))$

3. Compute $w_{t+1} = \sum_{i=1}^N p_{t+1,i} w_{t+1,i}$. Let f_{t+1} be $f(\cdot|\theta_t^{\text{feat}}, w_{t+1})$.

Output at time t : f'_{t+1} .

end for

B. Proof of Proposition 1

The proof of Proposition 1. We first write the derivation that $\sum_{y \in \mathcal{Y}} s_t[y] \cdot \nabla_f \mathbb{E}_{x \sim \mathcal{P}^{\text{train}}(\cdot|y)} \ell_{\text{sup}}(f_t(x), y)$ is an unbiased estimator of $\nabla_f \ell(f_t; \mathcal{P})$ when f_t is independent of S_t .

$$\begin{aligned} \mathbb{E}_{S_t} \left[\sum_{y \in \mathcal{Y}} s_t[y] \cdot \nabla_f \mathbb{E}_{x \sim \mathcal{P}^{\text{train}}(\cdot|y)} \ell_{\text{sup}}(f_t(x), y) \right] &= \sum_{y \in \mathcal{Y}} \mathbb{E}_{S_t} [s_t[y] \cdot \nabla_f \mathbb{E}_{x \sim \mathcal{P}^{\text{train}}(\cdot|y)} \ell_{\text{sup}}(f_t(x), y)] \\ &= \sum_{y \in \mathcal{Y}} \mathbb{E}_{S_t} [s_t[y]] \cdot \nabla_f \mathbb{E}_{x \sim \mathcal{P}^{\text{train}}(\cdot|y)} \ell_{\text{sup}}(f_t(x), y) \\ &= \sum_{y \in \mathcal{Y}} q_t[y] \cdot \nabla_f \mathbb{E}_{x \sim \mathcal{P}^{\text{train}}(\cdot|y)} \ell_{\text{sup}}(f_t(x), y) \\ &= \sum_{y \in \mathcal{Y}} q_t[y] \cdot \nabla_f \mathbb{E}_{x \sim \mathcal{P}_t^{\text{test}}(\cdot|y)} \ell_{\text{sup}}(f_t(x), y) \\ &= \nabla_f \ell(f_t; \mathcal{P}). \end{aligned}$$

The third equality is as how s_t is constructed. The fourth equality holds by the label shift assumption. We can check the second equality: if f_t is dependent of S_t , the correctness of the second equality is not guaranteed and so is the overall unbiased property derivation. \square

C. The Revision for Previous Online Label Shift Adaptation Algorithms

The revised algorithms to be used in the main algorithm OLS-OFU (Algorithm 1) are FTH-R (Algorithm 4), UOGD-R (Algorithm 5), ROGD-R (Algorithm 3), ATLAS-R (Algorithm 6).

D. Theorems for OLS and Proofs

In this section, we present the theoretical results of FLHFTL-OFU, ROGD-OFU, FTH-OFU, UOGD-OFU, ATLAS-OFU and their proofs. The proofs are mostly the same as the proofs for the original algorithms with small adjustments. As our results are not straight corollaries for the original theorems, we write the full proofs here for the completeness.

D.1. Theorem for FLHFTL-OFU

Before proving Theorem 2 (in Section 3.2) we recall the assumption from Baby et al. (2023) for convenience. We refer the reader to Baby et al. (2023) for justifications and further details of the assumptions.

Assumption 1. Assume access to the true label marginals $q_0 \in \Delta_K$ of the offline train data and the true confusion matrix $C \in \mathbb{R}^{K \times K}$. Further the minimum singular value $\sigma_{\min}(C) = \Omega(1)$ is bounded away from zero.

Assumption 2 (Lipschitzness of loss functions). Let \mathcal{D} be a compact and convex domain. Let r_t be any probabilistic classifier. Assume that $L_t(p) := E[\ell(g(\cdot; r_t, p/q_0)|x_t)]$ is G Lipschitz with $p \in \mathcal{D} \subseteq \Delta_K$, i.e, $L_t(p_1) - L_t(p_2) \leq G\|p_1 - p_2\|_2$ for any $p_1, p_2 \in \mathcal{D}$. The constant G need not be known ahead of time.

Theorem 2. [Regret convergence for FLHFTL-OFU] Suppose we choose the OLS subroutine in Algorithm 2 to be FLHFTL from Baby et al. (2023). Let $f_t^{\text{flhftl-ofu}}$ be the output at time step $t - 1$ from Algorithm 1, that is $g(\cdot; f_t'', \frac{q_t}{q_0})$. Let σ be the smallest among the the minimum singular values of invertible confusion matrices $\{C_{f_1'', D'_0}, \dots, C_{f_T'', D'_0}\}$. Then under Assumptions 1 and 2 in Baby et al. (2023), FLHFTL-OFU has the guarantee below:

$$\begin{aligned} & \mathbb{E} \left[\frac{1}{T} \sum_{t=1}^T \ell(f_t^{\text{flhftl-ofu}}; \mathcal{P}_t^{\text{test}}) - \frac{1}{T} \sum_{t=1}^T \ell(g(\cdot; f_t'', \frac{q_t}{q_0}); \mathcal{P}_t^{\text{test}}) \right] \\ & \leq O \left(\frac{K^{1/6} V_T^{1/3}}{\sigma^{2/3} T^{1/3}} + \frac{K}{\sigma \sqrt{T}} \right), \end{aligned} \quad (6)$$

where $V_T := \sum_{t=1}^T \|q_t - q_{t-1}\|_1$, K is the number of classes, and the expectation is taken w.r.t. randomness in the revealed co-variables. This result is attained without prior knowledge of V_T .

Proof:

The algorithm in Baby et al. (2023) requires that the estimate s_t in Line 1 of Algorithm 2 is unbiased estimate of the label marginal q_t . Since f_t'' in Algorithm 2 is independent of the sample S_t , and since we are working under the standard label shift assumption, due to Lipton et al. (2018) we have that $C_{f_t'', D'_0}^{-1} \cdot \frac{1}{|S_t|} \sum_{x_t \in S_t} f_t''(x_t)$ forms an unbiased estimate of $E_{x \sim \mathcal{P}_t^{\text{test}}}[f_t''(x)]$. Further, from Lipton et al. (2018), the reciprocal of standard deviation of this estimate is bounded below by minimum of the singular values of confusion matrices $\{C_{f_1'', D'_0}, \dots, C_{f_T'', D'_0}\}$.

Let \tilde{q}_t be the estimate of the label marginal maintained by FLHFTL. By Lipschitzness, we have that

$$E[\ell(f_t^{\text{flhftl-ofu}}; \mathcal{P}_t^{\text{test}}) - \ell(g(\cdot; f_t'', p/q_0))] = E[L_t(\tilde{q}_t)] - E[L_t(q_t)] \quad (9)$$

$$\leq G \cdot E[\|\tilde{q}_t - q_t\|_2], \quad (10)$$

where the last line is via Assumption 2.

$$\sum_{t=1}^T E[\ell(f_t^{\text{fhftl-ofu}}; \mathcal{P}_t^{\text{test}}) - \ell(g(\cdot; f_t'', p/q_0))] \leq \sum_{t=1}^T G \cdot E[\|\tilde{q}_t - q_t\|_2] \quad (11)$$

$$\leq \sum_{t=1}^T G \sqrt{E\|\tilde{q}_t - q_t\|_2^2} \quad (12)$$

$$\leq G \sqrt{T \sum_{t=1}^T E\|\tilde{q}_t - q_t\|_2^2} \quad (13)$$

$$= \tilde{O} \left(K^{1/6} T^{2/3} V_T^{1/3} (1/\sigma_{\min}^{2/3}(C)) + \sqrt{KT}/\sigma_{\min}(C) \right), \quad (14)$$

where the second line is due to Jensen's inequality, third line by Cauchy-Schwartz and last line by Proposition 16 in [Baby et al. \(2023\)](#). This finishes the proof.

D.2. Theorem for ROGD-OFU

We state the assumptions first for the later theorems. These assumptions are similar to Assumption 1-3 in [\(Wu et al., 2021\)](#).

Assumption 3. $\forall \mathcal{P} \in \{\mathcal{P}^{\text{train}}, \mathcal{P}_1^{\text{test}}, \dots, \mathcal{P}_T^{\text{test}}\}$, $\text{diag}(C_{f, \mathcal{P}})$ is differentiable with respect to f .

Assumption 4. $\forall t \in [T]$, $\ell(g(\cdot; f_t'', p/q_0); \mathcal{P}_t^{\text{test}})$ is convex in p , where f_t'' is defined in Algorithm 1.

Assumption 5. $\sup_{p \in \Delta^{K-1}, i \in [K], t \in [T]} \|\nabla_p \ell(g(\cdot; f_t'', p/q_0); \mathcal{P}_t^{\text{test}})\|_2$ is finite and bounded by L .

Theorem 3 (Regret convergence for ROGD-OFU). *If we run Algorithm 1 with ROGD-R (Algorithm 3) and $\eta = \sqrt{\frac{2}{T}} \frac{1}{L}$, under Assumption 3, 4, 5, ROGD-OFU satisfies the guarantee*

$$\mathbb{E} \left[\frac{1}{T} \sum_{t=1}^T \ell(f_t^{\text{ogd-ofu}}; \mathcal{P}_t^{\text{test}}) \right] - \min_{p \in \Delta_K} \mathbb{E} \left[\frac{1}{T} \sum_{t=1}^T \ell(g(\cdot; f_t'', p/q_0); \mathcal{P}_t^{\text{test}}) \right] \leq \sqrt{\frac{2}{T}} L. \quad (15)$$

$$\mathbb{E} \left[\frac{1}{T} \sum_{t=1}^T \ell(f_t^{\text{ogd}}; \mathcal{Q}_t) \right] - \min_{p \in \Delta_K} \mathbb{E} \left[\frac{1}{T} \sum_{t=1}^T \ell(g(\cdot; p, f_0, q_0); \mathcal{Q}_t) \right] \leq \sqrt{\frac{2}{T}} L. \quad (16)$$

Proof: For any fixed p ,

$$\begin{aligned} \ell(f_t^{\text{rogd-ofu}}; \mathcal{P}_t^{\text{test}}) - \ell(g(\cdot; f_t'', p/q_0); \mathcal{P}_t^{\text{test}}) &= \ell(g(\cdot; f_t'', p_t/q_0); \mathcal{P}_t^{\text{test}}) - \ell(g(\cdot; f_t'', p/q_0); \mathcal{P}_t^{\text{test}}) \\ &\leq (p_t - p) \cdot \nabla_p \ell(g(\cdot; f_t'', p_t/q_0); \mathcal{P}_t^{\text{test}}) \\ &= (p_t - p) \cdot J_{p, f_t''}(p_t)^\top \mathbb{E}_{S_t} [s_t | S_1, \dots, S_{t-1}] \\ &= \mathbb{E}_{S_t} [(p_t - p) \cdot J_{p, f_t''}(p_t)^\top s_t | S_1, \dots, S_{t-1}], \end{aligned}$$

where the last inequality holds by the fact that $(p_t - p) \cdot J_{p, f_t''}(p_t)^\top$ is independent of $\{S_1, \dots, S_{t-1}\}$. To bound $(p_t - p) \cdot J_{p, f_t''}(p_t)^\top s_t$,

$$\begin{aligned} \|p_{t+1} - p\|_2^2 &= \|\text{Prof}_{\Delta^{K-1}}(p_t - \eta \cdot J_{p, f_t''}(p_t)^\top s_t) - p\|_2^2 \\ &\leq \|p_t - \eta \cdot J_{p, f_t''}(p_t)^\top s_t - p\|_2^2 \\ &= \|p_t - p\|_2^2 + \eta^2 \|J_{p, f_t''}(p_t)^\top s_t\|_2^2 - 2\eta(p_t - p) \cdot (J_{p, f_t''}(p_t)^\top s_t). \end{aligned}$$

This implies

$$(p_t - p) \cdot (J_{p, f_t''}(p_t)^\top s_t) \leq \frac{1}{2\eta} (\|p_t - p\|_2^2 - \|p_{t+1} - p\|_2^2) + \frac{\eta}{2} \|J_{p, f_t''}(p_t)^\top s_t\|_2^2$$

Thus

$$\begin{aligned}
 & \mathbb{E}_{S_1, \dots, S_T} \left[\frac{1}{T} \sum_{t=1}^T \ell(f_t^{\text{rogd-ofu}}; \mathcal{P}_t^{\text{test}}) - \frac{1}{T} \sum_{t=1}^T \ell(g(\cdot; f_t'', p/q_0); \mathcal{P}_t^{\text{test}}) \right] \\
 & \leq \mathbb{E}_{S_1, \dots, S_T} \left[\frac{1}{T} \sum_{t=1}^T \frac{1}{2\eta} (\|p_t - p\|_2^2 - \|p_{t+1} - p\|_2^2) + \frac{\eta}{2} \|J_{p, f_t''}(p_t)^\top s_t\|_2^2 \right] \\
 & \leq \frac{1}{2\eta T} \|p_1 - p\|_2^2 + \frac{\eta}{2T} \sum_{t=1}^T \mathbb{E}_{S_1, \dots, S_t} [\|J_{p, f_t''}(p_t)^\top s_t\|_2^2] \\
 & \leq \frac{1}{\eta T} + \frac{\eta L^2}{2} = \sqrt{\frac{2}{T}} L.
 \end{aligned}$$

This bound holds for any p . Thus,

$$\mathbb{E}_{S_1, \dots, S_T} \left[\frac{1}{T} \sum_{t=1}^T \ell(f_t^{\text{rogd-ofu}}; \mathcal{P}_t^{\text{test}}) \right] - \min_{p \in \Delta^{K-1}} \mathbb{E}_{S_1, \dots, S_T} \left[\frac{1}{T} \sum_{t=1}^T \ell(g(\cdot; f_t'', p/q_0); \mathcal{P}_t^{\text{test}}) \right] \leq \sqrt{\frac{2}{T}} L.$$

D.3. Theorem for FTH-OFU

We begin with two assumptions.

Assumption 6. For any $\mathcal{P}^{\text{test}}$ s.t. $\mathcal{P}^{\text{test}}(x|y) = \mathcal{P}^{\text{train}}(x|y)$, denote $q_t := (\mathcal{P}_t^{\text{test}}(y = k) : k \in [K])$ and then

$$\|q_t - \arg \min_{p \in \Delta^{K-1}} \ell(g(\cdot; f_t'', p/q_0); \mathcal{P}^{\text{test}})\| \leq \delta.$$

Assumption 7. $\forall \mathcal{P}^{\text{test}}$ s.t. $\mathcal{P}^{\text{test}}(x|y) = \mathcal{P}^{\text{train}}(x|y)$, $\sup_p \|\nabla_p \ell(g(\cdot; f_t'', p/q_0); \mathcal{P}^{\text{test}})\| \leq L$

Theorem 4 (Regret convergence for FTH-OFU). *If we run Algorithm 1 with FTH-R (Algorithm 4) and assume σ is no larger than the minimum singular value of invertible confusion matrices $\{C_{f_1'', D_0}, \dots, C_{f_T'', D_0}\}$, under Assumption 6 and 7 with $\delta = 0$, FTH-OFU satisfies the guarantee that with probability at least $1 - 2KT^{-\tau}$ over samples $S_1 \cup \dots \cup S_T$,*

$$\frac{1}{T} \sum_{t=1}^T \ell(f_t^{\text{fth-ofu}}; \mathcal{P}_t^{\text{test}}) - \min_{p \in \Delta^K} \frac{1}{T} \sum_{t=1}^T \ell(g(\cdot; f_t'', p/q_0); \mathcal{P}_t^{\text{test}}) \leq O\left(\frac{\log T}{T} + \frac{1}{\sigma} \sqrt{\frac{K \log T}{T}}\right), \quad (17)$$

where K is the number of classes.

Proof: Denote $q_t := (\mathcal{P}_t^{\text{test}}(y = k) : k \in [K])$. By the Hoeffding and union bound, we have

$$\mathbb{P}\left(\forall t \leq T, \|p_{t+1} - \frac{1}{t} \sum_{\tau=1}^t q_\tau\| \leq \sqrt{K} \varepsilon_t\right) \geq 1 - \sum_{t=1}^T 2M \exp(-2\varepsilon_t^2 t / \sigma^2).$$

This implies that with probability at least $1 - \sum_{t=1}^T 2M \exp(-2\varepsilon_t^2 t / \sigma^2)$, $\forall p$,

$$\begin{aligned}
 & \sum_{t=1}^T \ell(p_t; \mathcal{P}_t^{\text{test}}) - \sum_{t=1}^T \ell(g(\cdot; f_t'', p/q_0); \mathcal{P}_t^{\text{test}}) \\
 & \leq \sum_{t=1}^T \ell(g(\cdot; f_t'', \frac{1}{t} \sum_{\tau=1}^t q_\tau / q_0); \mathcal{P}_t^{\text{test}}) - \sum_{t=1}^T \ell(g(\cdot; f_t'', p/q_0); \mathcal{P}_t^{\text{test}}) + L\sqrt{M} \cdot \sum_{t=1}^T \varepsilon_t \\
 & \leq \sum_{t=1}^T \ell(g(\cdot; f_t'', \frac{1}{t-1} \sum_{\tau=1}^{t-1} q_\tau / q_0); \mathcal{P}_t^{\text{test}}) - \sum_{t=1}^T \ell(g(\cdot; f_t'', \frac{1}{t} \sum_{\tau=1}^t q_\tau / q_0); \mathcal{P}_t^{\text{test}}) + L\sqrt{M} \cdot \sum_{t=1}^T \varepsilon_t \\
 & \leq \sum_{t=1}^T L \left\| \frac{1}{t-1} \sum_{\tau=1}^{t-1} q_\tau - \frac{1}{t} \sum_{\tau=1}^t q_\tau \right\| + L\sqrt{M} \cdot \sum_{t=1}^T \varepsilon_t \\
 & \leq \sum_{t=1}^T \frac{L}{t} \left\| \frac{1}{t-1} \sum_{\tau=1}^{t-1} q_\tau - q_t \right\| + L\sqrt{M} \cdot \sum_{t=1}^T \varepsilon_t \\
 & \leq \sum_{t=1}^T \frac{2L}{t} + L\sqrt{M} \cdot \sum_{t=1}^T \varepsilon_t.
 \end{aligned}$$

If we take $\varepsilon_t = 2\sigma \sqrt{\frac{\ln T}{T}}$, the above is equivalent to: with probability at least $1 - 2KT^{-7}$

$$\frac{1}{T} \sum_{t=1}^T \ell(p_t; \mathcal{P}_t^{\text{test}}) - \min_p \frac{1}{T} \sum_{t=1}^T \ell(g(\cdot; f_t'', p/q_0); \mathcal{P}_t^{\text{test}}) \leq 2L \frac{\ln T}{T} + 4L\sigma \sqrt{\frac{K \ln T}{T}}$$

D.4. Theorems for UOGD-OFU and ATLAS-OFU

Theorem 5. [Regret convergence for UOGD-OFU] Let $f(\cdot; \theta_{f_t''}^{\text{feat}}, w)$ denote a network with the same feature extractor as that of f_t'' and a last linear layer with weight w . Let $f^{\text{uogd-ofu}} = f(\cdot; \theta_{f_t''}^{\text{feat}}, w_t)$, where w_t is the weight maintained at round t by Algorithm 5. If we run Algorithm 1 with UOGD in (Bai et al., 2022) and let step size be η , then under the same assumptions as Lemma 1 in (Bai et al., 2022), UOGD-OFU satisfies that

$$\mathbb{E} \left[\frac{1}{T} \sum_{t=1}^T \ell(f^{\text{uogd-ofu}}; \mathcal{P}_t^{\text{test}}) - \frac{1}{T} \sum_{t=1}^T \min_{w \in \mathcal{W}} \ell(f(\cdot; \theta_{f_t''}^{\text{feat}}, w); \mathcal{P}_t^{\text{test}}) \right] \leq O \left(\frac{K\eta}{\sigma^2} + \frac{1}{\eta T} + \sqrt{\frac{V_{T,\ell}}{T\eta}} \right), \quad (18)$$

where $V_{T,\ell} := \sum_{t=2}^T \sup_{w \in \mathcal{W}} |\ell(f(\cdot; \theta_{f_t''}^{\text{feat}}, w); \mathcal{P}_t^{\text{test}}) - \ell(f(\cdot; \theta_{f_{t-1}''}^{\text{feat}}, w); \mathcal{P}_{t-1}^{\text{test}})|$, σ denotes the minimum singular value of the invertible confusion matrices $\{C_{f_1'', D_0}, \dots, C_{f_T'', D_0}\}$ and K is the number of classes and the expectation is taken with respect to randomness in the revealed co-variates.

Proof Sketch: Recall that $\ell(f(\cdot; \theta_{f_t''}^{\text{feat}}, w); \mathcal{P}_t^{\text{test}}) := E_{(x,y) \sim \mathcal{P}_t^{\text{test}}} \ell_{\text{ce}}(f(x|\theta_{f_t''}^{\text{feat}}, w), y)$.

This guarantee follows from the arguments in Bai et al. (2022) from two basic facts below:

1. The risk $\ell(f(\cdot; \theta_{f_t''}^{\text{feat}}, w); \mathcal{P}_t^{\text{test}})$ is convex in w over a convex and compact domain \mathcal{W} .
2. It is possible to form unbiased estimates $\hat{G}_t(w) \in \mathbb{R}^K$ such that $E[\hat{G}_t(w)|S_{1:t-1}] = E_{((x,y) \sim \mathcal{P}_t^{\text{test}})} \nabla_w \ell_{\text{ce}}(f(x|\theta_{f_t''}^{\text{feat}}, w), y)$.

Hence we proceed to verify these two facts in our setup. Fact 1 is true because the cross-entropy loss is convex in any subset of the simplex and the last linear layer weights only defines an affine transformation which preserves convexity.

For fact 2, note that the f_t'' only uses the data until round $t-1$. So by the same arguments in Bai et al. (2022), using the BBSE estimator defined from the classifier f_t'' , the unbiased estimate of risk gradient can be defined.

Let w_t be the weight of the last layer maintained by UOGD at round t . Let $u_{1:T}$ be any sequence in \mathcal{W} . Consequently we have for any round,

$$\ell(f^{\text{uogd-ofu}}; \mathcal{P}_t^{\text{test}}) - \ell(f(\cdot; \theta_{f_t'}^{\text{feat}}, u_t)) = \ell(f(\cdot; \theta_{f_t'}^{\text{feat}}, w_t) - \ell(f(\cdot; \theta_{f_t'}^{\text{feat}}, u_t)) \quad (19)$$

$$\leq \langle \nabla_w \ell(f(\cdot; \theta_{f_t'}^{\text{feat}}, w_t), w_t - u_t) \rangle \quad (20)$$

$$= \langle E[\hat{G}_t(w_t) | S_{1:t-1}], w_t - u_t \rangle. \quad (21)$$

Rest of the proof is identical to [Bai et al. \(2022\)](#).

Theorem 6 (Regret convergence for ATLAS-OFU). *Let $f(\cdot; \theta_{f_t'}^{\text{feat}}, w)$ denote a network with the same feature extractor as that of f_t'' and a last linear layer with weight w . Let $f^{\text{atlas-ofu}} = f(\cdot; \theta_{f_t'}^{\text{feat}}, w_t)$, where w_t is the weight maintained at round t by Algorithm 6. If we run Algorithm 1 with ATLAS in ([Bai et al., 2022](#)) and set up the step size pool $\mathcal{H} = \{\eta_i = O\left(\frac{\sigma}{\sqrt{KT}}\right) \cdot 2^{i-1} | i \in [N]\}$ ($N = 1 + \lceil \frac{1}{2} \log_2(1 + 2T) \rceil$), then under the same assumptions as Lemma 1 in ([Bai et al., 2022](#)), UOGD-OFU satisfies that*

$$\mathbb{E} \left[\frac{1}{T} \sum_{t=1}^T \ell(f^{\text{atlas-ofu}}; \mathcal{P}_t^{\text{test}}) - \frac{1}{T} \sum_{t=1}^T \min_{w \in \mathcal{W}} \ell(f(\cdot; \theta_{f_{t+1}'}^{\text{feat}}, w); \mathcal{P}_t^{\text{test}}) \right] \leq O \left(\left(\frac{K^{1/3}}{\sigma^{2/3}} + 1 \right) \frac{V_{T,\ell}^{1/3}}{T^{1/3}} + \sqrt{\frac{K}{\sigma^2 T}} \right), \quad (22)$$

where $V_{T,\ell} := \sum_{t=2}^T \sup_{w \in \mathcal{W}} |\ell(f(\cdot; \theta_{f_t'}^{\text{feat}}, w); \mathcal{P}_t^{\text{test}}) - \ell(f(\cdot; \theta_{f_{t-1}'}^{\text{feat}}, w); \mathcal{P}_{t-1}^{\text{test}})|$, σ denotes the minimum singular value of the invertible confusion matrices $\{C_{f_1', D'_0}, \dots, C_{f_T', D'_0}\}$ and K is the number of classes and the expectation is taken with respect to randomness in the revealed co-variates.

The proof is similar to that of Theorem 5 and hence omitted.

Discussion about the assumption. In the theorems for UOGD and ATLAS, the definition of $V_{T,\ell}$ is shift severity from $\mathcal{P}_t^{\text{test}}$. However, in the theorems for UOGD-OFU and ATLAS-OFU above, $V_{T,\ell}$ is shift severity from both $\mathcal{P}_t^{\text{test}}$ and $\theta_{f_t'}^{\text{feat}}$, which can be much larger. This might lead to harder convergence of the regret.

E. Additional experiments

E.1. Additional details of datasets

Severity of CIFAR-10C in the experiment. For each type of corruption in CIFAR-10C, we select a mild level and a high level of severity in the experiment section. Here we introduce the exact parameters of mild and high levels of severity for those corruptions. For Gaussian Noise, the severity levels for [mild, high] are [0.03, 0.07]. For Fog, the severity levels for [mild, high] are [(0.75, 2.5), (1.5, 1.75)]. For Pixelate, the severity levels for [mild, high] are [0.75, 0.65].

Details of additional datasets. In addition to CIFAR-10 and CIFAR-10C, we evaluate on three more datasets: STL10 ([Coates et al., 2011](#)), CINIC ([Darlow et al., 2018](#)), and EuroSAT ([Helber et al., 2019](#)). Similar to CIFAR-10, we split the original train sets of these datasets into the train set and the validation set by the ratio 4 : 1 and use the original test sets for sampling test images in the online test stage.

E.2. Results on Additional Datasets

Figure 2(b) and Figure 5 show the results for three additional datasets: STL10, CINIC, and EuroSAT, also with OLS-OFU (rotation degree prediction) under sinusoidal shift setting. In-line with CIFAR-10, we observe that OLS and OLS-OFU can perform better than Base and OFU, and OLS-OFU can outperform OLS. We find this pattern to be more consistent for EuroSAT and STL10 than CINIC.

E.3. More Results on CIFAR-10

Figure 6 shows the results on CIFAR-10 for Bernoulli shift cross three SSL methods in OLS-OFU. Similar to Figure 2(a), OLS-OFU within all three SSL methods outperforms all baseline methods.

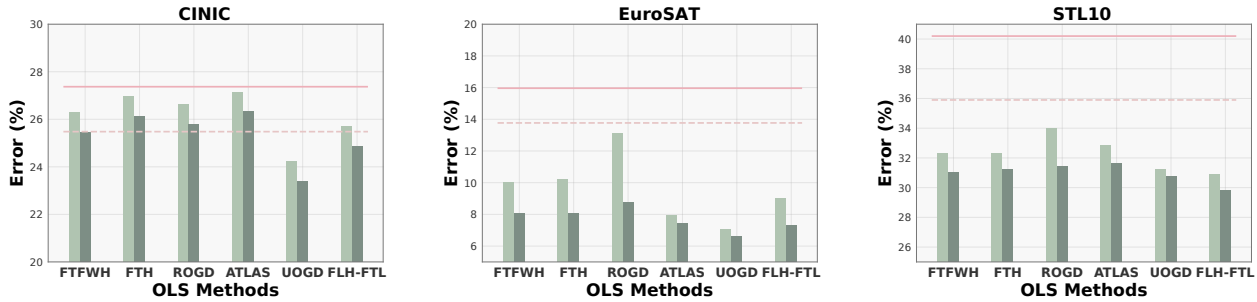


Figure 5. Results on three more datasets. SSL in OLS-OFU is rotation degree prediction and online shift pattern is Bernoulli shift.

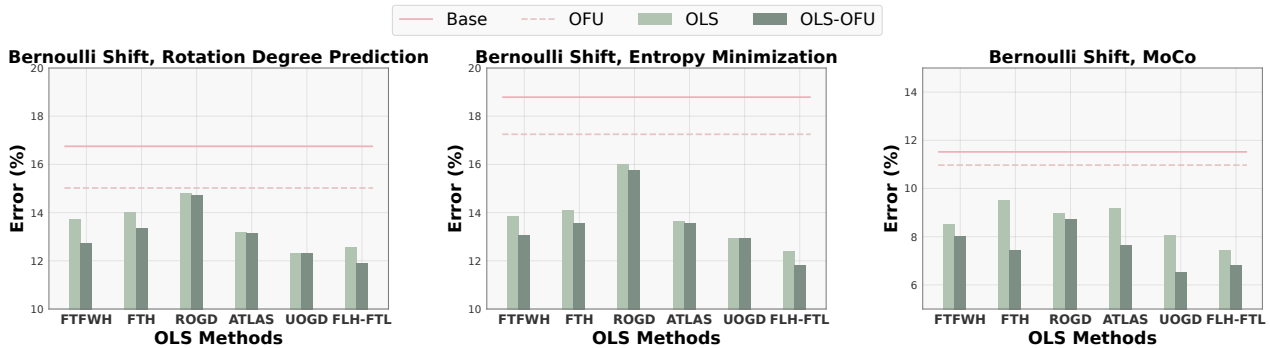


Figure 6. Results of Bernoulli shifts on CIFAR-10. OLS-OFU is evaluated with three SSL methods.

E.4. More Results on CIFAR-10C

We evaluate three SSL methods in OLS-OFU on CIFAR-10C for two online shift patterns. We pick moderately high severity levels for evaluating CIFAR-10C. In Figure 7 we can observe the consistent improvement from OLS to OLS-OFU and the SOTA performance of OLS-OFU.

E.5. More Results on CIFAR-10C with High Severity

We evaluate three SSL methods in OLS-OFU on CIFAR-10C with *high severity* for two online shift patterns. In Figure 8, we can observe when SSL in OLS-OFU is rotation degree prediction or MoCo, the improvement from OLS to OLS-OFU is very significant but OLS-OFU cannot outperform OFU. The conclusion is similar to the discussion for Figure 4 in Section 4. However, OLS-OFU with SSL entropy minimization has different behavior. When the corruption of CIFAR-10C becomes more severe, OLS-OFU entropy minimization shows less improvement from OLS, if we compare the transition: Figure 7 (clean CIFAR-10), Figure 7 (CIFAR-10C with mild severity), Figure 8 (CIFAR-10C with high severity). This suggests that rotation degree prediction and MoCo are more appropriate SSL to address the domain shift from CIFAR-10 to CIFAR-10C.

E.6. Empirical evaluation for Equation 8

Figure 9 shows the comparison between LHS (OLS-OFU) and RHS (OLS) of the inequality in Equation 8 when the SSL in OLS-OFU is entropy minimization or MoCo. Similar to what we observe in Figure 3, the inequality in Equation 8 holds cross 4 data settings and two online shift patterns when OLS-OFU is implemented with entropy minimization or MoCo.

E.7. Ablation for the order of updates and predictions

In the default framework of online distribution shift as shown in Figure 1, the model updates happen after the predictions for the samples at time step t . We would like to see if the model updated before the predictions would bring benefit. Figure 10 shows the comparison between "predict first" and "update first". We can observe that there is no strong evidence to demonstrate the advantage of "predict first" or "update first" – the difference is indeed insignificant. However, because in

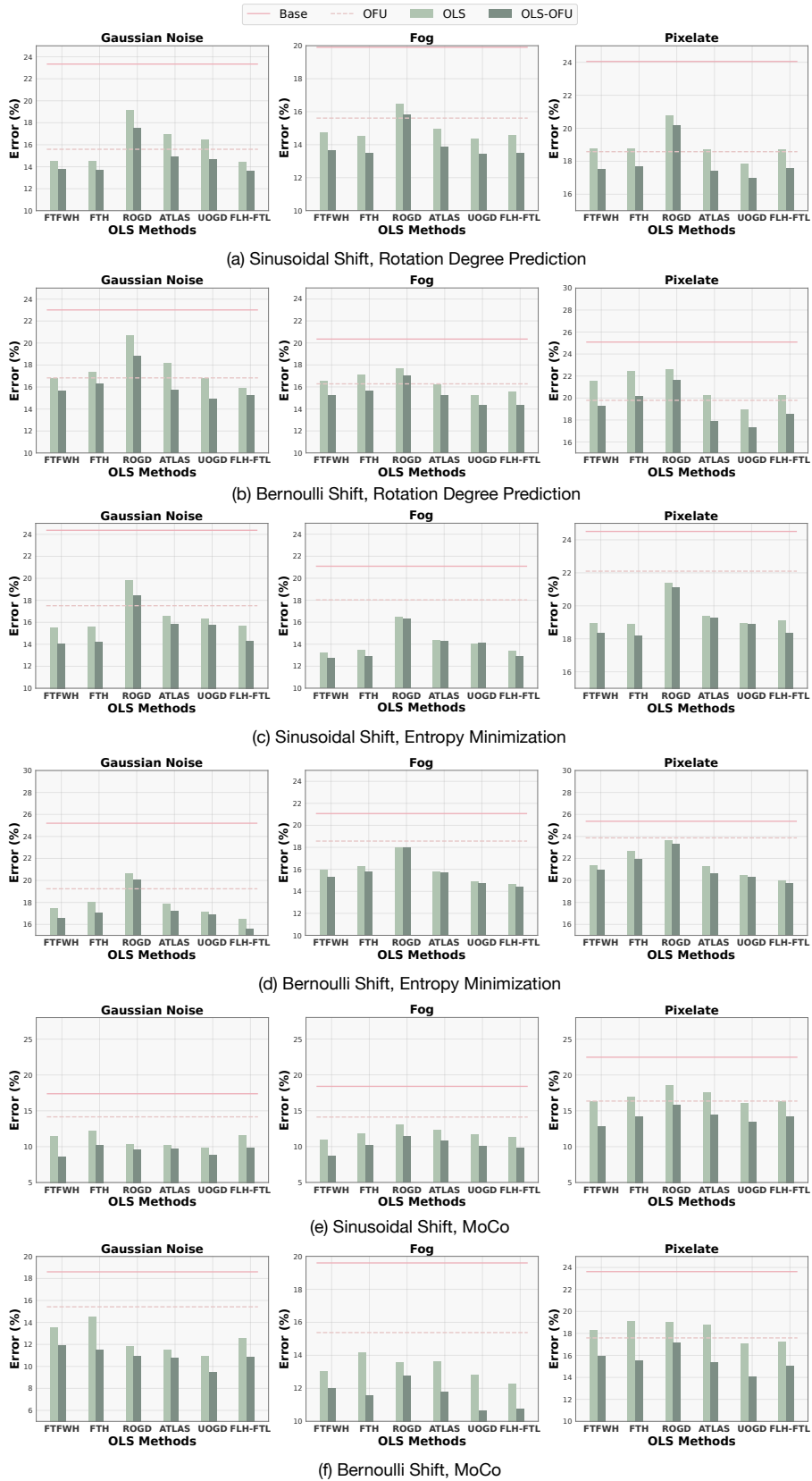


Figure 7. Results of two online shift patterns on CIFAR-10C and three SSL methods in OLS-OFU.

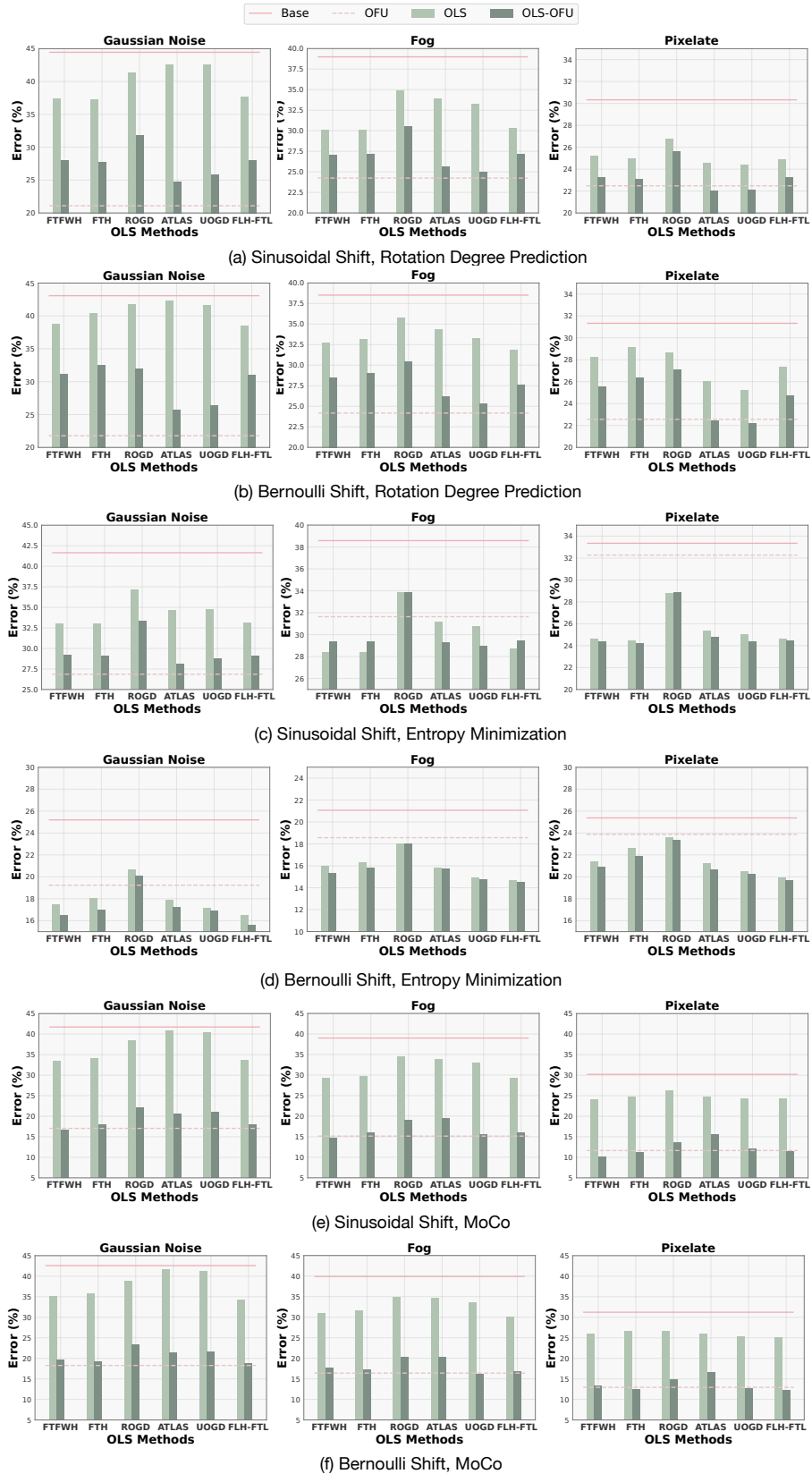


Figure 8. Results of two online shift patterns on CIFAR-10C (high severity) and three SSL methods in OLS-OFU.

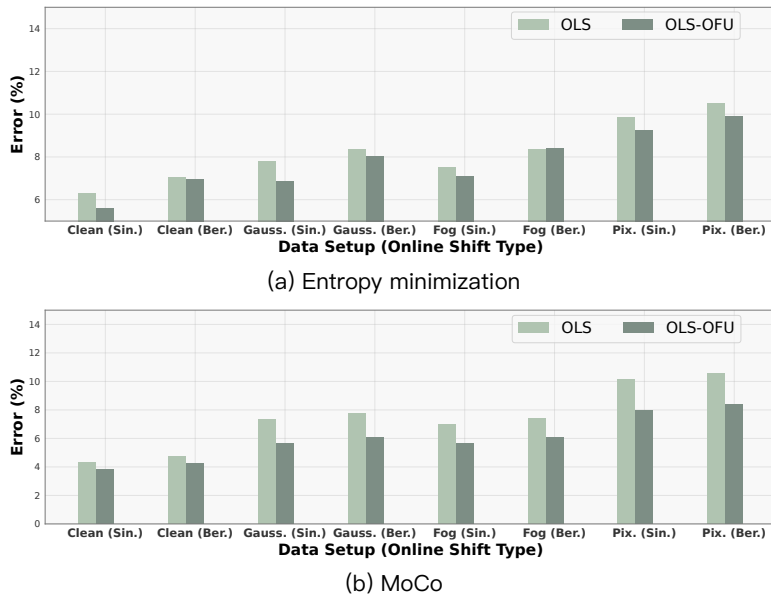


Figure 9. Sanity check for the inequality $\mathbb{E} \left[\frac{1}{T} \sum_{t=1}^T \ell(g(\cdot; f_t'', q_t/q_0); \mathcal{P}_t^{\text{test}}) \right] < \frac{1}{T} \sum_{t=1}^T \ell(g(\cdot; f_0, q_t/q_0); \mathcal{P}_t^{\text{test}})$ (Equation 8) when SSL in OLS-OFU is entropy minimization or MoCo.

the framework of ”predict first” OLS and OLS-OFU enjoy strong theoretical guarantees, we recommend ”predict first” in practice.

E.8. Details of SSL Methods

When the SSL loss is rotation degree prediction, it requires another network f^{deg} to predict the rotation degree, sharing the same feature extractor θ^{feat} as f_0 but with a different set of downstream layers. Its SSL loss $\ell_{\text{ssl}}(S; f)$ is defined as $\sum_{x \in S} \ell_{ce}(f^{\text{deg}}(R(x, i)), i)$, where i is an integer uniformly sampled from $[4]$, and $R(x, i)$ is to rotate x with degree $\text{DL}[i]$ from a list of degrees $\text{DL} = [0, 90, 180, 270]$. Alternatively, if the SSL loss is entropy minimization, $\ell_{\text{ssl}}(S; f)$ would be the entropy $\sum_{x \in S} \sum_{k=1}^K f(x)_k \log f(x)_k$. Moreover, the SSL loss would be a contrastive loss (InfoNCE) where the positive example x' is an augmented version of x and other samples in the same time step can be the negative examples. However, the batch size for a time step is small, e.g. 10 in our experiment. MoCo updates with such a small batch won’t work. Thus, we experiment with MoCo by applying a batch accumulation strategy, which we introduce next.

E.8.1. BATCH ACCUMULATION FOR MOCO

Prior test-time training (rotation degree prediction, entropy minimization) methods operate with the OFU framework easily, with feature extractor updates taking place in each time step. Rotation degree prediction originates as a self-supervised training method (Gidaris et al., 2018), thus naturally we evaluate more recent self-supervised training methods, namely MoCo (He et al., 2020; Chen et al., 2020b; 2021). No prior work shows how to use MoCo (or self-supervised learning in general) in a test-time training setting. Given that self-supervised training is sensitive to batch size, the intuition is that a larger batch size (much larger than the number of online samples available per time step) is required to perform a valid gradient update for a MoCo checkpoint. As such, we evaluated a *batch accumulation* strategy OLS-OFU (BA= τ), where we continue evaluating online samples per time step, but only perform the online feature update at every τ steps (having accumulated the online samples throughout the τ steps in one batch). In particular, we perform feature extractor update every $\tau = 50$ steps (for 1000 steps, feature update occurs 20 times, online samples evaluation occurs 1000 times), evaluating with 10 online samples per time step, using a smaller learning rate (0.0005) but test-time train with 10 epochs. Notice that $\tau = 1$ is the default setting in Algorithm 1. OLS-OFU with MoCo presented in Figure 2, Figure 6 and Figure 7 is equivalent to OLS-OFU (BA=50).

To show the necessity of large τ , we evaluate both OLS-OFU (BA=1) and OLS-OFU (BA=50) on CIFAR-10 (Figure 11) and CIFAR-10C (Figure 12). Firstly, we can observe that OLS-OFU (BA=1) is even worse than OLS. We hypothesize this is

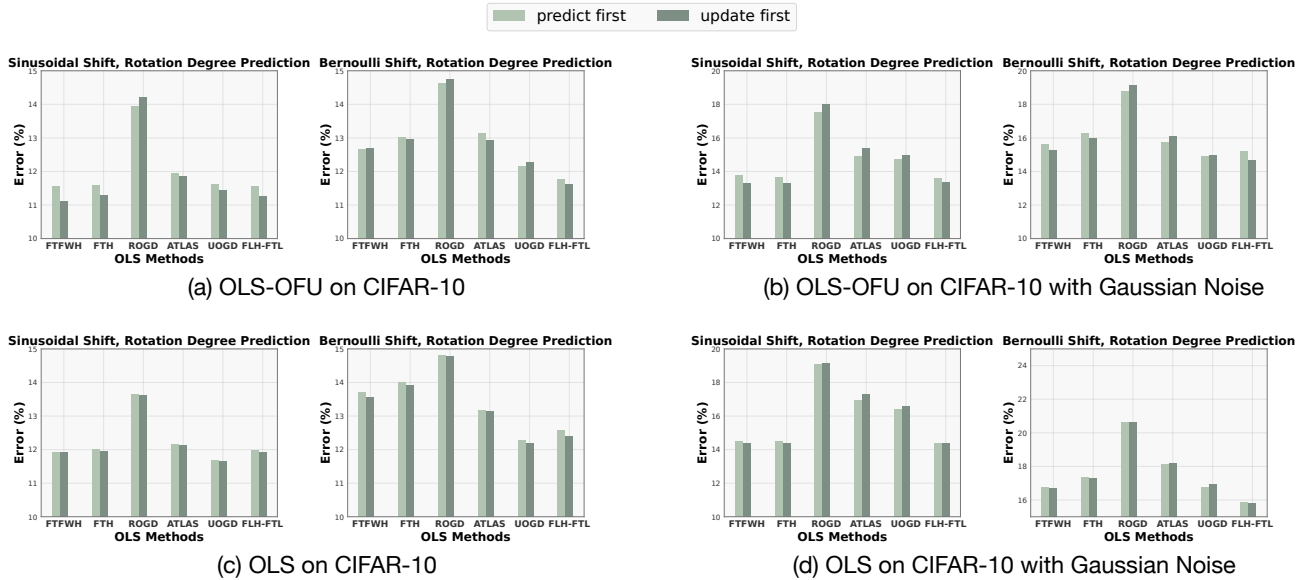


Figure 10. Ablation for the order of updates and predictions.

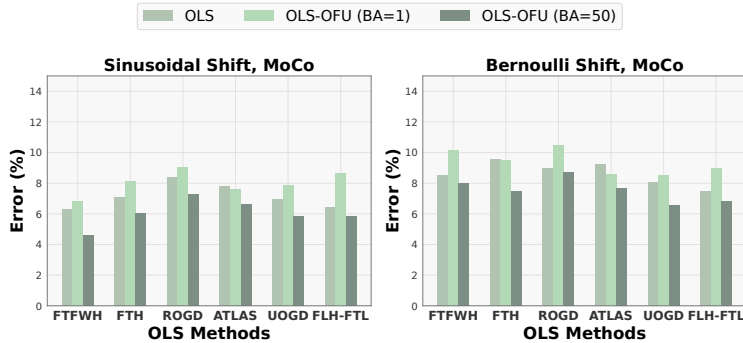


Figure 11. Evaluating OLS-OFU with different batch accumulations for MoCo on CIFAR-10.

because small batch size of MoCo will hurt the performance and larger batch size in MoCo is necessary. Hence, we increase τ from 1 to 50 and then we can observe the significant improvement from OLS-OFU (BA=1) to OLS-OFU (BA=50). Now, OLS-OFU (BA=50) can outperform OLS.

E.9. Improvements compared with literature

We would like to compare the improvements in the literature for the OLS problem and the improvements from the SOTA in the literature to our method OLS-OFU. We can calculate the difference Δ_{error} between the errors of method A and B to show the improvement $A \rightarrow B$. To measure the improvements in the literature for the OLS problem, we measure Δ_{error} between FTH (proposed in the first OLS paper) and FLHFTL (SOTA in the literature). We also calculate Δ_{error} between FLHFTL and FLHFTL-OFU.

Figure 13 shows the Δ_{error} for FTH \rightarrow FLHFTL and FLHFTL \rightarrow FLHFTL-OFU across all data settings (dataset and online shift pattern) when the SSL in OFU is set as rotation degree prediction. The improvement of FLHFTL \rightarrow FLHFTL-OFU is as significant as the improvement of FTH \rightarrow FLHFTL. Moreover, the improvement of FLHFTL \rightarrow FLHFTL-OFU is more consistent. This consistency demonstrates the potential that OLS-OFU can have improvement for any future OLS algorithm.

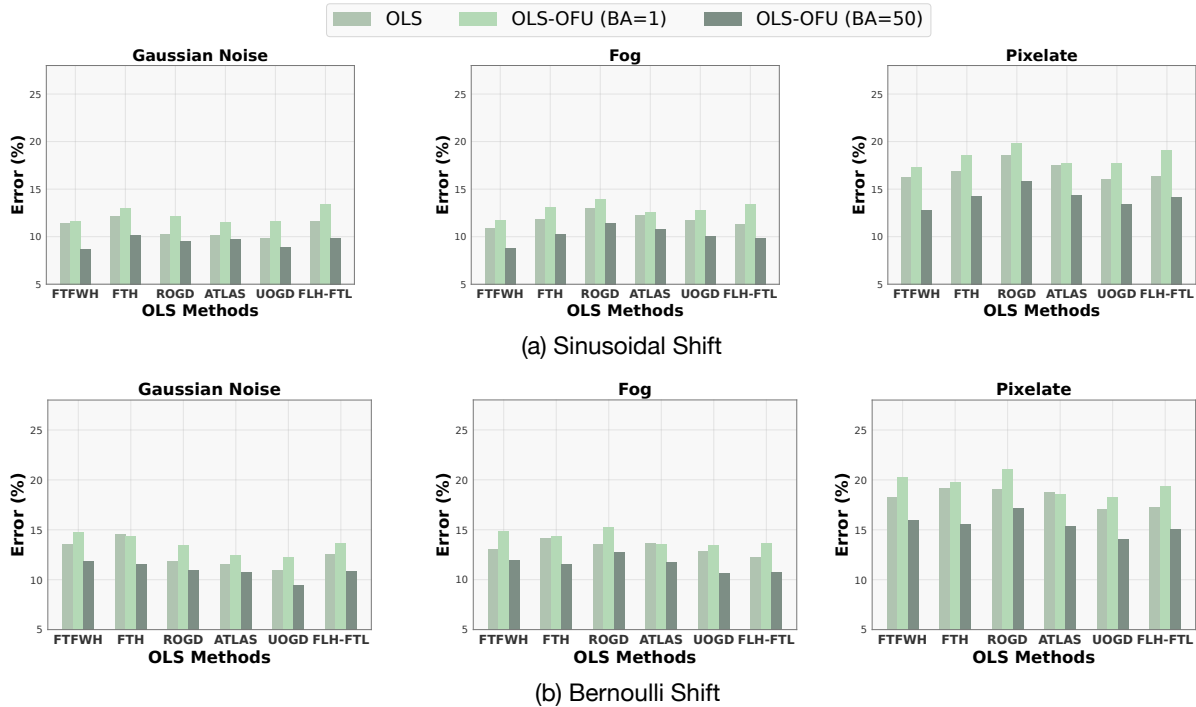


Figure 12. Evaluating OLS-OFU with different batch accumulations for MoCo on CIFAR-10C.

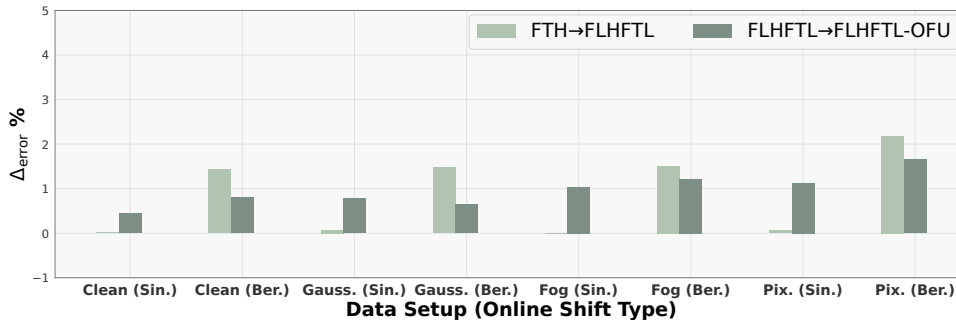


Figure 13. Improvements from FTH to FLHFTL and improvements from FLHFTL to FLHFTL-OFU across all datasets and online shift patterns.

E.10. Self-training

Pseudo labelling (Lee, 2013), a common self-training technique, generates pseudo labels for unlabelled data and uses them to update the model. Though we are not able to use ground-truth labels to compute feature extractor updates, we can use the model at time t to make predictions with respect to the online samples at time t , and train on the inputs with their assigned (pseudo) labels. An issue that arises in self-training is confirmation bias, where the model repeatedly overfits to incorrect pseudo-labels. As such, different methods can be used to select which samples will be pseudo-labelled and used in updating the model, e.g. using data augmentation (Arazo et al., 2020), using regularization to induce confident low-entropy pseudo-labelling (Grandvalet & Bengio, 2004a), using softmax thresholds to filter out noisy low-confidence predictions (Xie et al., 2020). We make use of ensembles to identify noisy low-confidence/entropy pseudo-label predictions, though other various alternatives can also be used. In addition to OLS and OLS-OFU, we highlight the methods under comparison:

- *OLS-OFU* ($\ell_{\text{sup}}(\cdot, y_{\text{ground-truth}})$): Instead of computing pseudo-labels, we make use of the correct ground-truth labels $y_{\text{ground-truth}}$. Recall ℓ_{sup} is the supervised learning loss. We update the feature extractor with the supervised loss w.r.t.

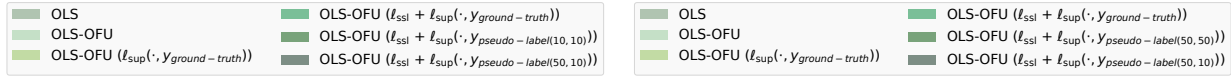
ground-truth labels $\ell_{\text{sup}}(\cdot, y_{\text{ground-truth}})$.

- *OLS-OFU* ($\ell_{\text{ssl}} + \ell_{\text{sup}}(\cdot, y_{\text{ground-truth}})$): Instead of computing pseudo-labels, we make use of the correct ground-truth labels $y_{\text{ground-truth}}$. Recall ℓ_{ssl} and ℓ_{sup} are the self-supervised and supervised learning losses respectively. We update the feature extractor with both the self-supervised loss ℓ_{ssl} as well as the supervised loss w.r.t. ground-truth labels $\ell_{\text{sup}}(\cdot, y_{\text{ground-truth}})$.
- *OLS-OFU* ($\ell_{\text{ssl}} + \ell_{\text{sup}}(\cdot, y_{\text{pseudo-label}(\#\text{samples}=\cdot, \#\text{FU-samples}=\cdot))$): Recall ℓ_{ssl} and ℓ_{sup} are the self-supervised and supervised learning losses respectively. We compute pseudo-labels $y_{\text{pseudo-label}}$, and update the feature extractor with both the self-supervised loss ℓ_{ssl} as well as the supervised loss w.r.t. pseudo-labels $\ell_{\text{sup}}(\cdot, y_{\text{pseudo-label}})$.

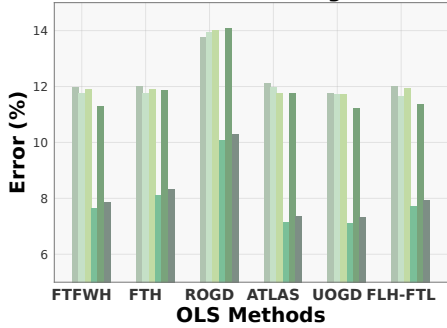
How to compute pseudo-labels? We now describe the procedure to compute pseudo-labels for $\ell_{\text{sup}}(\cdot, y_{\text{pseudo-label}(\#\text{samples}=\cdot, \#\text{FU-samples}=\cdot)})$. The seed used to train our model is 4242, and we train an additional 4 models on seeds 4343, 4545, 4646, 4747. With this ensemble of 5 models, we keep sampling inputs at each online time step until we have $\#\text{FU-samples}$ samples, or we reach a limit of $\#\text{samples}$ samples. We accept an input when the agreement between the ensembles exceeds a threshold $e = 1.0$ (i.e. we only accept samples where all 5 ensembles agree on the label of the online sample). In the default online learning setting, there are only $\#\text{samples}=10$, and therefore there may not be enough accepted samples to perform feature update with, thus we evaluate with a continuous sampling setup, where we sample $\#\text{samples}=50$ (and evaluate on all these samples), but only use the first 10 samples ($\#\text{FU-samples}=10$) to perform the feature extractor update.

Results on pseudo-labelling. First, we find that *OLS-OFU* ($\ell_{\text{ssl}} + \ell_{\text{sup}}(\cdot, y_{\text{ground-truth}})$) attains the lowest error and is the lower bound we are attaining towards. Evaluating *OLS-OFU* ($\ell_{\text{ssl}} + \ell_{\text{sup}}(\cdot, y_{\text{pseudo-label}(\#\text{samples}=10, \#\text{FU-samples}=10)})$), we find that the performance does not outperform OLS-OFU, and is not near *OLS-OFU* ($\ell_{\text{ssl}} + \ell_{\text{sup}}(\cdot, y_{\text{ground-truth}})$). If we set the threshold e too high, there may not be enough online samples to update the feature extractor. If we set the threshold e too low, there may be too many incorrect labels and we incorrectly update our feature extractor. As such, we would like to sample more inputs at each online time step such that we can balance this tradeoff. We sample $\#\text{samples}=50$ at each online time step, and update with $\#\text{FU-samples} \leq 10$. For fair comparison, we also show the comparable methods in both $\#\text{samples}=10, \#\text{FU-samples}=10$ and $\#\text{samples}=50, \#\text{FU-samples}=50$ settings.

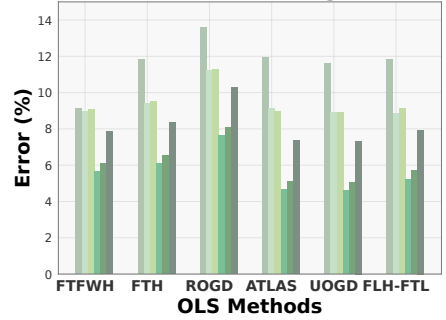
With this sampling setup, we find that *OLS-OFU* ($\ell_{\text{ssl}} + \ell_{\text{sup}}(\cdot, y_{\text{pseudo-label}(\#\text{samples}=50, \#\text{FU-samples}=10)})$) can outperform both *OLS-OFU* ($\#\text{samples}=10$) and *OLS-OFU* ($\#\text{samples}=50$). Though it does not exceed neither *OLS-OFU* ($\ell_{\text{ssl}} + \ell_{\text{sup}}(\cdot, y_{\text{ground-truth}})$) for $\#\text{samples}=10$ nor $\#\text{samples}=50$, it lowers the gap considerably.



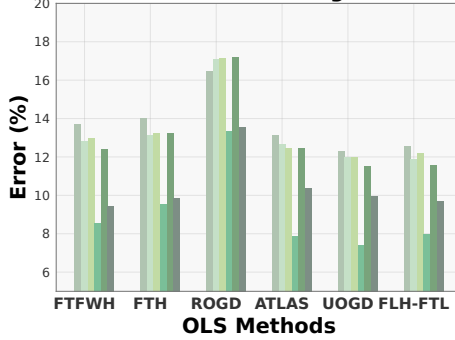
Sinusoidal Shift, Rotation Degree Prediction



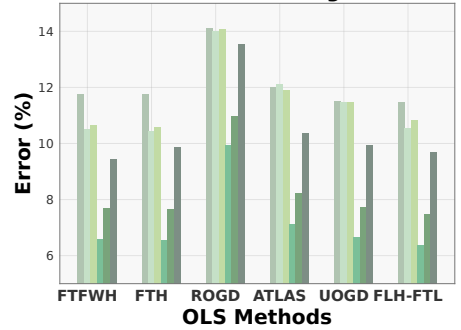
Sinusoidal Shift, Rotation Degree Prediction



Bernoulli Shift, Rotation Degree Prediction



Bernoulli Shift, Rotation Degree Prediction



(a) number of online samples: 10

(b) number of online samples: 50

Figure 14. Results on pseudo-labelling.